Quaternary Science Reviews 239 (2020) 106364

Contents lists available at ScienceDirect

Quaternary Science Reviews

journal homepage: www.elsevier.com/locate/quascirev

Last Glacial Maximum environmental conditions at Andøya, northern Norway; evidence for a northern ice-edge ecological "hotspot"

Inger G. Alsos [a, *], Per Sjögren [a], Antony G. Brown [a, b], Ludovic Gielly [c], Marie Kristine Føreid Merkel [a], Aage Paus [d, e], Youri Lammers [a], Mary E. Edwards [a, b], Torbjørn Alm [a], Melanie Leng [f], Tomasz Goslar [g], Catherine T. Langdon [b], Jostein Bakke [e, h], Willem G.M. van der Bilt [e, h]

[a] UiT – The Arctic University of Norway, Tromsø Museum, N-9037, Tromsø, Norway
[b] University of Southampton, Geography and Environmental Science, Southampton, SO17 1BJ, UK
[c] Laboratoire d'Ecologie Alpine (LECA), Université Grenoble Alpes, C2 40700 38058, Grenoble, Cedex 9, France
[d] University of Bergen, Department of Biological Science, N-5020, Bergen, Norway
[e] The Bjerknes Centre for Climate Research, Bergen, Norway
[f] British Geological Survey, Centre for Environmental Geochemistry, Nottingham, NG12 5GG, UK
[g] Faculty of Physics, Adam Mickiewicz University, Poznan, Poland
[h] University of Bergen, Department of Earth Science, N-5020, Bergen, Norway

ARTICLE INFO

Article history:
Received 5 February 2020
Received in revised form
5 May 2020
Accepted 6 May 2020
Available online 5 June 2020

Keywords:
Ancient DNA (*a*DNA)
Andøya
Climate variability
Environmental conditions
Glacial survival
Last glacial maximum
Late Weichselian
MIS2
Micro-refugia
Sedimentary DNA (*sed*DNA)

ABSTRACT

Andøya on the NW coast of Norway is a key site for understanding the Last Glacial Maximum (LGM) in northern Europe. Controversy has arisen concerning the local conditions, especially about the timing and extent of local glacial cover, maximum July temperatures and whether pine and/or spruce could have grown there. We reviewed all existing data and add newly analysed ancient sedimentary DNA (*sed*aDNA), pollen, macrofossils, geochemistry and stable isotopes from three lake sediment cores from Øvre Æråsvatnet. A total of 23 new dates and age-depth modelling suggests the lake has been ice-free since GI2 (<23.4 cal ka BP) and possibly GS3 (<26.7 cal ka BP). *Pinus* and *Picea sed*aDNA was found in all three cores but at such low frequencies that it could not be distinguished from background contamination. LGM samples have an exceptionally high organic matter content, with isotopic values indicating that carbon and nitrogen derive from a marine source. Along with finds of bones of the little auk (*Alle alle*), this indicates that the lake received guano from an adjacent bird colony. *Sed*aDNA, pollen and macrofossil assemblages were dominated by Poaceae, Brassicaceae and *Papaver*, but scattered occurrence of species currently restricted to the Low Arctic Tundra Zone (July temperature of 8–9 °C) such as Apiaceae (*sed*aDNA, 8–9 °C), and *Alchemilla alpina* (macrofossil, 8–9 °C) were also recorded. The review of >14.7 cal ka BP data recorded 94 vascular plant taxa, of which 38% have a northern limit in Shrub Tundra or more southern vegetation zones. This unusual assemblage likely stems from a combination of proximity to ice-free water in summer, geographical isolation linked with stochastic long-distance dispersal events, and the presence of bird-fertilized habitats. The environmental reconstruction based on all records from the area does not preclude local growth of tree species, as the local climate combined with high nutrient input may have led to periodically suitable environmental 'hotspot' conditions.

© 2020 The Authors. Published by Elsevier Ltd. This is an open access article under the CC BY license (http://creativecommons.org/licenses/by/4.0/).

1. Introduction

Evidence for cryptic glacial-age refugia, or micro-refugia, in the northern hemisphere has long been sought but remains elusive (Birks and Willis, 2008; Brochmann et al., 2003; Stewart and Lister, 2001; Tzedakis et al., 2013), despite the fact that phylogenetic data strongly suggest they may have existed (Anderson et al., 2006; Napier et al., 2020; Westergaard et al., 2019). It is likely that late-glacial tundra zones supported small populations of boreal trees in Alaska (Brubaker et al., 2005), Yukon (Zazula et al., 2006), Siberia (Binney et al., 2009; Tarasov et al., 2009), and Estonia (Heikkilä

* Corresponding author.
E-mail address: inger.g.alsos@uit.no (I.G. Alsos).

https://doi.org/10.1016/j.quascirev.2020.106364
0277-3791/© 2020 The Authors. Published by Elsevier Ltd. This is an open access article under the CC BY license (http://creativecommons.org/licenses/by/4.0/).

et al., 2009). It remains highly controversial, however, whether tree taxa grew within the maximum limits of the Scandinavian ice sheet (Birks et al., 2005; Kullman, 2005), as is indicated by megafossils of spruce and pine in the Scandinavian mountains (Kullman, 2002), and sedimentary ancient DNA (*seda*DNA) in lake sediments from a glacial refugium at Andøya (Birks et al., 2012a; Parducci et al., 2012a, 2012b). As all proxies for reconstructing past flora and environmental conditions have some uncertainties, a multi-proxy study may provide more robust conclusions. Environmental reconstructions are often focused on temperature (Birks and Birks, 2014; Trondman et al., 2015), but temperature may interact with other key drivers, such as nutrient cycling: high nutrient levels may compensate for low temperature, as seen, for example, at high-latitude bird cliffs (González-Bergonzoni et al., 2017). Thus, estimation of nutrient availability and trophic status may further elucidate the environmental conditions in refugia and may be critical for micro-refugia.

The northern Norwegian island of Andøya is a key locality for understanding LGM environments (here defined as the 26-18 cal ka BP interval) on the North Atlantic margin (Vorren, 1978), and it has been extensively studied. Andøya is situated where the Norwegian continental shelf is at its narrowest (under 10 km). Due to calving into the deep ocean, there was no possibility of thick ice build-up, and the area became deglaciated early (Hughes et al., 2016; Patton et al., 2017). While higher elevations on northern parts of Andøya remained ice-free throughout the LGM (Nesje et al., 2007), it is less clear whether the lowland was continuously ice-free from ca. 26 ca. ka BP (Alm, 1993; Vorren and Plassen, 2002; Vorren et al., 2013, 2015).

Palaeobotanical investigations have been carried out on three lakes on the northern ice-free tip of Andøya (Fig. 1): Endletvatn (Alm and Elverland, 2012; Elverland, 2012; Elverland and Alm, 2012; Parducci et al., 2012b; Vorren, 1978; Vorren and Alm, 1999; Vorren et al., 2013), Nedre Æråsvatnet (Alm and Birks, 1991; Vorren et al., 1988) and Øvre Æråsvatnet (Alm, 1993). The late-glacial vegetation recorded as pollen and plant macrofossils, combined with slow minerogenic sedimentation, has been assumed to typify cold and dry polar desert conditions (*sensu lato*). There may, however, have been interruptions: warmer periods when mean July temperatures reached up to 10 °C, as indicated by features such as high concentrations/accumulation rates of pollen and/or macrofossils and the occasional presence of more thermophilous plant taxa (Alm, 1993; Alm and Birks, 1991; Elverland and Alm, 2012; Vorren, 1978). Recently, *seda*DNA of pine and spruce of LGM age was found (Parducci et al., 2012b). The discovery of conifer *seda*DNA on Andøya was unexpected, and it was debated as to whether the origin was due to contamination, long-distance pollen, driftwood, re-sedimentation, or possibly in-situ growth (Birks et al., 2012a; Parducci et al., 2012a, 2012b). The debate was further stirred by Vorren et al. (2013) who, based on both new and re-interpreted data, concluded that LGM mean July temperatures never exceeded 3 °C. This interpretation would preclude any tree growth during the LGM on Andøya, but it is primarily based on the inference that the combination of the dominant moss species *Syntrichia ruralis* and *Aulacomnium turgidum* found as macrofossils represent Polar Desert vegetation, and it contradicts previous palaeoecological interpretations of past climatic conditions (Alm, 1993; Alm and Birks, 1991; Elverland and Alm, 2012; Parducci et al., 2012a, 2012b; Vorren, 1978). It follows that the chronology, environmental conditions and palaeoecology of N Andøya warrant further clarification.

This study seeks to capitalize on recent advances in both the methodology (laboratory procedures, bioinformatics pipeline) and understanding of sedimentary ancient DNA to: **1**) more precisely date the ice-free period, **2**) evaluate the pine and spruce *seda*DNA results from Parducci et al. (2012b) by investigating a second lake on Andøya using improved methods; **3**) assess the local LGM palaeoenvironment based on additional proxy records, including stable isotopes, and **4**) review previous investigations, with special emphasis on environmental conditions and the potential for tree growth on Andøya during the LGM.

2. Regional setting

At Andøya (Fig. 1), the proximity of the continental shelf to abyssal depths (6.1 km from the coast to the top of the Andøya Canyon; Laberg et al., 2000) limited the vertical extent of glaciers during the Weichselian glaciation, and therefore the island was deglaciated early compared with other sites along the western seaboard (Vorren et al., 2015). This is in line with recent work on continental glaciation that suggests that topography/trough geometry had an overriding effect on glacial extent and recession rates (Small et al., 2018). The tip of Andøya is also crossed by ice-marginal deposits which Vorren and Plassen (2002) associated with the Egga I (before 24 cal ka BP) and Egga II (23-22.2 cal ka BP) deposits at the shelf edge (Vorren et al., 2015).

Andøya's northern tip is an important site for LGM palaeoenvironmental studies because its lakes received sediment input at this time. This study targets Øvre Æråsvatnet (69°15′22″N; 16°02′03″E). The basin sits at 43 m a.s.l, a few meters above the local LGM marine limit. The lake has inlets to the W and SW and an outlet to the NE (Fig. 1). The July mean temperature is 11 °C, and the February mean is −2.2 °C; average annual precipitation is 1060 mm (Norwegian Metrological Institute; eKlima 2016; 1961–1990). The lake covers 20.4 ha, similar to the areas of two adjacent lakes, Nedre Æråsvatnet (20.6 ha, 34 m a.s.l.) and Endletvatn (28.6 ha, 35 m a.s.l.; Fig. 1). The lake is surrounded by birch forest and mires and there is planted spruce and pine, especially on the south-facing slope of Store Æråsen. The bedrock is entirely non-calcareous (amphibolites, hornblende and mica-gneisses, Norwegian Geological Survey Database), and the catchment size is 3.6 km^2.

3. Material and methods

3.1. Field work

Lake Øvre Ærsåsvatnet was chosen because, in contrast to Endletvatn, where conifer *seda*DNA was previously detected (Parducci et al., 2012), it is above the marine limit and therefore less likely to have received driftwood. Fieldwork was conducted early in March 2014 when the lake was covered by ice. A north-south transect across the lake was test-cored using a Hiller sampler (And5-And7 and And9, Fig. 2). The laminated gyttja of expected LGM age (Alm, 1993) was only found in samples from the shallower, south-central part of the lake. To further assess sediment distribution and water depth, we surveyed the basin with Ground Penetrating Radar (GPR). For this purpose, we used a Malå GPR setup fitted with an unshielded 50 MHz antenna. The rough terrain antenna was dragged behind a snow scooter at constant speed (10 km/h) while traversing the lake in semi-regular grids. Following acquisition, all data were processed in version 1.4 of the RadExplorer software package with a set of prescribed band-pass filtering, DC removal and time-zero adjustment routines. We then traced the interfaces between water, sediment and bedrock based on these optimized GPR reflections. Finally, all data were exported to ArcMap 10.4 to construct maps and models. Coring was conducted with a Geonor piston corer (110 mm diameter) and a modified Nesje corer (110 mm; (Nesje, 1992; Paus et al., 2015). Only

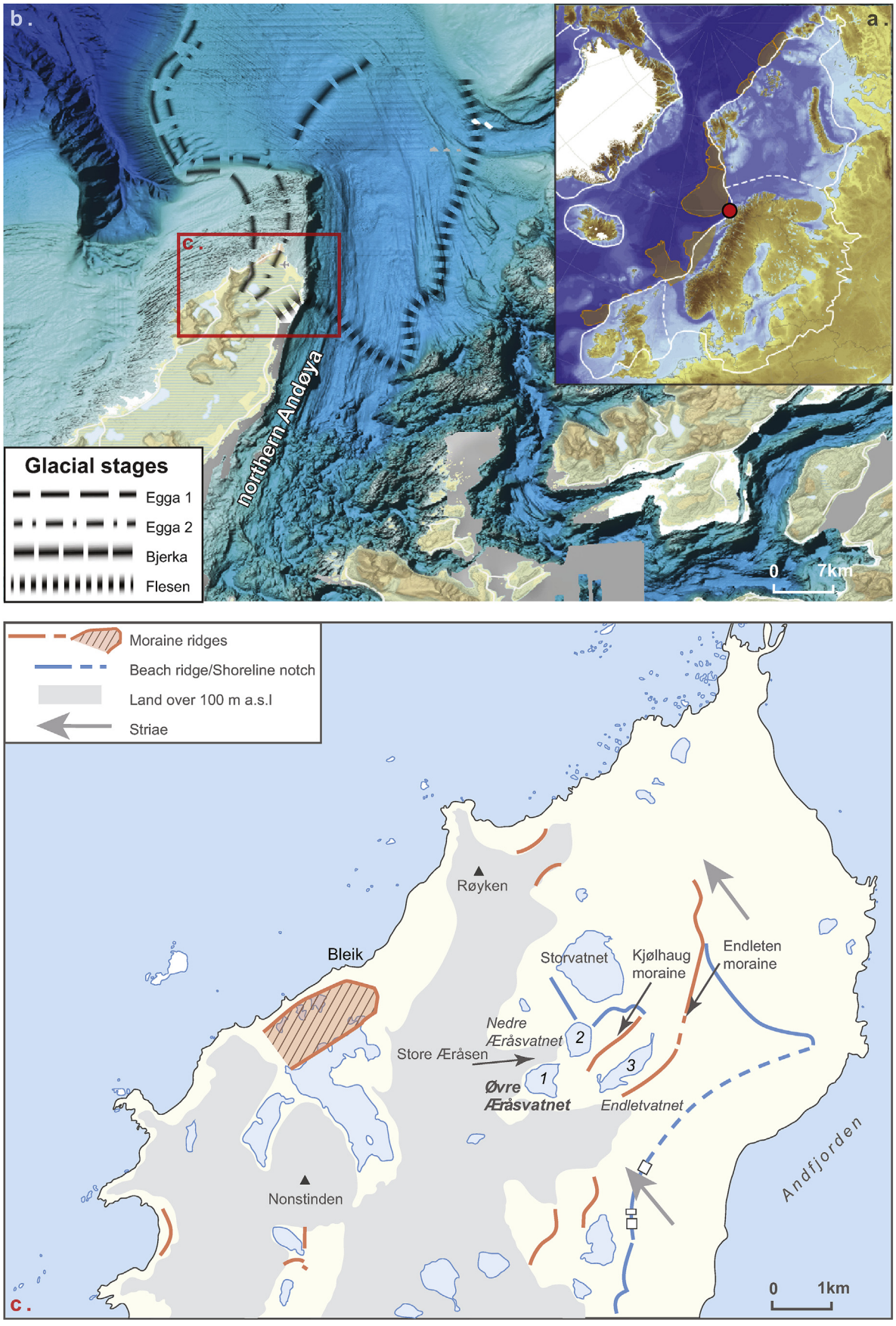

Fig. 1. A: Map of northern Eurasia with LGM ice limits (white line) and trough-mouth fans (brown fields) after Hughes et al. (2016). The location of Andøya is highlighted with a red dot. **B**: The northern part of the island Andøya with surrounding region (modified from norgeskart.no). Glacial stages (Vorren et al., 2015) discussed in the text are highlighted by stippled and dashed lines. **C**: Close-up of Lake Øvre Æråsvatnet and the surrounding lakes, as well as local moraines and coastal landforms (Vorren et al., 2015) discussed in the text. Numbers mark previous investigations: 1) Alm, 1993; 2) Vorren et al. (1988); Alm and Birks (1991); 3) Vorren (1978); Vorren and Alm (1999); Alm and Elverland (2012); Elverland (2012); Elverland and Alm (2012); Parducci et al. (2012b); Vorren et al. (2013); Vorren and Alm (1999). (For interpretation of the references to colour in this figure legend, the reader is referred to the Web version of this article.)

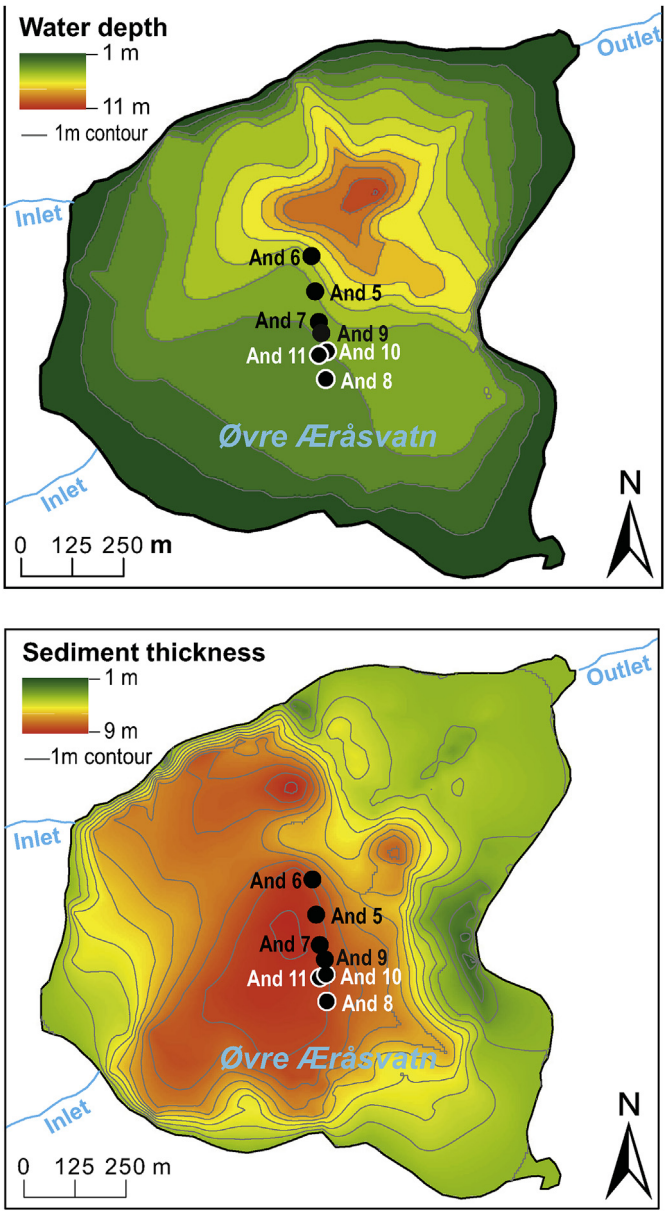

Fig. 2. Bathymetry and sediment thickness map of Lake Øvre Æråsvatnet showing also the test cores (And5-7, And9) and sediment cores (And-8, and-10 and And11).

the deepest part of the lake-sediment package was collected. A 3.46-m continuous core was retrieved with the modified Nesje-corer (And-11, 69.25579°N, 16.03517°E; 3.15 m water, total depth 11.88 m; subsequently divided in three parts). Two shorter cores taken with the Geonor corer (And-8, 3.15 m water, total depth 11.98 m, core length 1.14 m; And-10, 69.25552°N, 16.03516°E, 2.9 m water, total depth 10.16 m, core length 1.16 m) were collected 5 m west and 30 m south, respectively, from And-11 (Fig. 2).

3.2. Radiocarbon dating

The radiocarbon ages of 23 identified plant macrofossils were determined using Accelerator Mass Spectrometry at Poznan Radiocarbon Laboratory (Poz; Table 1). The bulk of the dated material consisted of bryophytes (moss stems), but seeds and leaf fragments of vascular plants were included when available. Low mass ($\leq$ 0.2 mg) of many samples led to relatively large uncertainties, but this was preferred to combining more material. The values for $\delta^{13}C$ are given in Table 1 but are inaccurate due to having been measured with the AMS, and the unusually low $\delta^{13}C$ values reported for the smallest samples were related to the extremely small amounts of carbon available for analysis. It is notable that all the $\delta^{13}C$ values are under −19. If the samples were contaminated with old C, or marine C, the values would be expected to be higher. The ^{14}C ages were calibrated with OxCal 4.2 (Bronk Ramsey, 2009) using IntCal13 (Reimer et al., 2013), and age-depth modelling was undertaken using Bacon v. 2.3.9.1 (Blaauw and Christen, 2011).

3.3. Geochemical analyses

Colour line-scan images with a resolution of approximately 70 μm were acquired using a Jai L-107CC 3 CCD RGB Line Scan Camera fitted on an Avaatech XRF core scanner (Fig. 3). Qualitative element-geochemical analyses were carried out with the XRF core scanner. The measurements were carried out at continuous 10-mm steps. Instrument settings were 10 kV, 1000 μA, 10 s count time, and no filter. Data processing was performed using WinAxil version 4.5.6. To minimize the influence of water and matrix effects (Tjallingii et al., 2007; Weltje and Tjallingii, 2008), the results are presented as ratios of selected elements divided by the sum of the 7 most abundant elements (Ca, Cl, Fe, K, S, Si and Ti; Rhodium (Rh) not included as it is induced by the equipment). Loss-on-ignition (LOI) was analysed every 4 cm. About 10 g of sediment was dried overnight at 105 °C, weighed, and then burned for 4 h at 550 °C. LOI was calculated as the percent dry-weight loss after burning.

Thirty samples were selected from the And-11 core for $\delta^{13}C$ and $\delta^{15}N$ analysis and determination of %C and %N. The isotope analyses were conducted in the Stable Isotope Facility at the British Geological Survey, UK. Samples for carbon isotopes were decarbonated in 5% HCl prior to analysis while a separate aliquot for nitrogen isotopes was run without pre-treatment. $\delta^{13}C$ analyses were performed by combustion in a Costech ECS4010 Elemental Analyser (EA) on-line to a VG TripleTrap (plus secondary cryogenic trap) and Optima dual-inlet mass spectrometer, with $\delta^{13}C$ values calculated to the VPDB scale using a within-run laboratory standard (BROC2) calibrated against external standards NBS-19 and NBS-22. Replicate analysis of well-mixed samples indicate an analytical precision of ± <0.1‰ (1 SD). Percent C and N analyses were run at the same time, and calibrated against an Acetanilide standard. $\delta^{15}N$ analyses were performed by combustion in a Thermo Finnigan Flash EA (1112 series) on-line to a Delta Plus XL mass spectrometer. $\delta^{15}N$ was calculated to the $\delta^{15}N$ value of air using the internal BROC2 standard calibrated against UGS40 and UGS41. Replicate analysis of well mixed samples indicated a precision of ±<0.2‰ (1 SD).

3.4. sedaDNA analysis

The DNA analyses of these sediments proved challenging, and we repeated the whole process three times. For the first extraction, we followed the phosphate buffer extraction protocol of Taberlet et al., (2012). While this works well for modern soil samples, we had poor results (as with other ancient samples). We then tried the PowerMax extraction kit (MO BIO Laboratories, Carlsbad, CA, USA), a method that has worked well for other sediments (Alsos et al., 2016; Clarke et al., 2019). Here, the results were also poor. We suspect that the main problem was the high organic content of the lower part of core And-11 and all of And-8 and And-10, as we have experienced similar problems with other highly organic sediments (Clarke et al., 2018). The uppermost, less organic part of core And-11 yielded reasonable results in all three analyses. For the third extraction, we used sterile plastic tools for taking 74 samples from

Table 1
Radiocarbon dates. Weight of dated material is added when this is so low that it might influence the probability estimate.

Core	Depth	Lab #	^{14}C BP (1σ)	Cal. BP (2 σ)	Cal. BP (2 σ) median	δ13C	Material
And-11	848 cm	Poz-72236	7320 ± 50	8300–8010	8155	−33.2	Moss, plant mat., leaves (0.2 mg)
And-11	916 cm	Poz-72235	9520 ± 50	11090–10660	10875	−33.3	Moss, plant mat., leaves (0.2 mg)
And-11	968 cm	Poz-77608	10120 ± 120	12150–11260	11705	−21.8	Moss (0.06 mg)
And-11	980 cm	Poz-72234	10770 ± 80	12800–12570	12685	−33.7	Moss, leaves (0.2 mg)
And-11	993 cm	Poz-72233	10900 ± 60	12930–12690	12730	−30.0	Moss (*Warnstorfia fluitans*)
And-11	1020 cm	Poz-72231	12530 ± 80	15130–14300	14715	−19.2	Moss, seeds
And-11	1052 cm	Poz-72230	12750 ± 90	15550–14830	15190	−20.7	Moss, seeds (0.2 mg)
And-11	1084 cm	Poz-72229	13120 ± 110	16070–15340	15705	−18.6	Moss, seeds, plant mat.
And-11	1096 cm	Poz-77610	16670 ± 150	20510–19710	20110	−22.1	Moss, seeds (0.14 mg)
And-11	1100 cm	Poz-104680	12880 ± 190	16019–14673	15346	−29.2	Moss stems (0.06 mg)
And-11	1112 cm	Poz-104682	14180 ± 250	17891–16501	17196	−44.1	Seed case (0.05 mg)
And-11	1128 cm	Poz-72219	16610 ± 110	20360–19710	20030	−26.9	Moss, seeds
And-11	1136 cm	Poz-104683	19060 ± 130	23364–22579	22972	−37.3	Moss stems (0.18 mg)
And-11	1156 cm	Poz-77611	17390 ± 150	21450–20590	21020	−27.6	Moss, seeds (0.2 mg)
And-11	1160 cm	Poz-104684	12120 ± 500	13760–11110	12435	−37.3	Herb stem fragments (0.02 mg)
And-11	1181 cm	Poz-77656	22410 ± 120	27120–26330	26725	−25.3	Moss
And-8	1090 cm	Poz-72215	12630 ± 100	15310–14420	14865	−31.8	Moss, seeds (0.2 mg)
And-8	1122 cm	Poz-77607	11930 ± 180	14280–13370	13825	−19.4	Moss, seeds (0.02 mg)
And-8	1134 cm	Poz-72214	15840 ± 200	19610–18720	19165	−46.7	Moss, seeds, plant mat. (0.14 mg)
And-8	1182 cm	Poz-72213	17840 ± 230	22230–20980	21605	−50.5	Moss, seeds (0.11 mg)
And-10	908 cm	Poz-72217	16120 ± 190	19940–18980	19460	−40.4	Moss, seeds (0.13 mg)
And-10	960 cm	Poz-77606	16180 ± 210	20040–19000	19520	−19.3	Moss, seeds (0.06 mg)
And-10	1004 cm	Poz-72216	16990 ± 240	21150–19910	20530	−43.4	Moss, seeds (0.08 mg)

the three cores. We extracted *sedaDNA* using an adapted version of Zimmermann et al. (2017), in which we downscaled the input volume to ~0.3 g, substituted the Qiagen PowerMax kit for the PowerSoil PowerLyzer kit, and incorporated a bead beating step following Alsos et al. (2016). We included negative controls during sampling (n = 2), extraction (n = 4), transferring extract from tubes to plates (n = 2), PCR setup (n = 2), and post-PCR (n = 2), as well as a synthetic positive control (n = 2), in total 14 controls. Here we only present data from the third extraction.

During this study, the dedicated ancient DNA laboratory of the Tromsø museum was moved twice between buildings and all reagents were replaced; the three runs exhibited different background contamination levels. We did detect pine (*Pinus*) and spruce (*Picea*) in all three runs, both in samples and in negative controls, but there were inconsistencies within samples.

For all three runs, the short and variable P6 loop region of the chloroplast trn*L* (UAA) intron (Taberlet et al., 2007) was used as diagnostic marker, following the same analysis protocol (Alsos et al., 2016; Sjögren et al., 2017), and running 8 PCR replicates on each DNA extract. The PCR replicates were pooled, cleaned and quantified with Qubit (Invitrogen™ Quant-iT™ and Qubit™ dsDNA HS Assay Kit, Thermofisher). The pools were converted into DNA libraries using a Truseq DNA PCR-free low throughout library prep kit (Illumina). The library was quantified by qPCR using the KAPA Library Quantification Kit for Illumina sequencing platforms (Roche) and a Prism 7500 Real Time PCR System (Life Technologies, Fisheries faculty, UiT). The library was normalised to a working concentration of 10 nM using the molarity calculated from qPCR adjusted for fragment size. Sequencing was on an Illumina HiSeq 2000 platform (2 × 150 bp, mid-output mode, dual indexing) at the Genomics Support Centre Tromsø (UiT).

All next-generation sequence data were aligned, filtered and trimmed using the OBITools software package (Boyer et al., 2016) using similar criteria as Alsos et al. (2016) and Sjögren et al. (2017). Resulting barcodes were assigned to taxa using the *ecotag* program (Yoccoz, 2012) and two independent reference datasets. One reference contained regional arctic and boreal sequences (Soininen et al., 2015; Sønstebø et al., 2010; Willerslev et al., 2014) and the other the NCBI nucleotide database (January 2018 release). The resulting identifications were merged and filtered, retaining barcode sequences if they: 1) were identified to 100% in either reference set; 2) were present in at least 3 PCR replicates from the same sample (hereafter referred to as PCR repeats); and 3) had at least 10 reads across the entire dataset. We removed the likely false positives relating to common PCR errors and food contaminants, based on experience from the analyses of 15 other sediment cores at Tromsø Museum, as well as taxa identified above family level (Supplementary Table S1). In our final step of filtering, we compared the frequency of sequences in PCR repeats in all 76 samples to the 10 negative controls. There is no clear way to set the cut-off (Alsos et al., 2018; Sjögren et al., 2017), so we chose a conservative value, keeping only sequences that had an overall frequency of PCR repeats in samples at least twice as high as in that in negative controls. We present the data semi-quantitatively as the proportion of PCR repeats, excluding replicates that had no DNA.

3.5. Pollen and macrofossils

Pollen analysis was attempted on 19 samples from the And-11 core in the depth range 910–1182 cm. Residual material from *sedaDNA* extraction 1 was used. As we resampled the core for *sedaDNA* extraction 3, minor stratigraphic differences between pollen and *sedaDNA* samples are possible. Every second or third level analysed for *sedaDNA* in extraction 3 corresponds to a pollen sample, except 1038 cm, which was only analysed for pollen. Pollen samples (1 cm^3) were prepared (Palaeoecological laboratory, University of Southampton) using conventional methods (Berglund and Ralska-Jasiewiczowa, 1986) and mounted in silicon oil. Counting was undertaken by CL and AP. Identifications were based on Fægri and Iversen (1989) and Moore et al. (1991), in combination with reference collections of modern material. In the two uppermost levels (910, 918 cm), the dryland pollen sums were 260 and 134; otherwise pollen sums were <100 grains, and often very low. In four samples the pollen sum was <10. However, we retained them to prevent imposing false negatives and because two of the records contained pine pollen which is a theoretical source of pine DNA.

Macrofossils were collected from 44 levels from core And-11 across the depth range 884–1181 cm. Slices ~2-cm thick were sampled every 8 cm (from half the core width, ca. 50 ml volume),

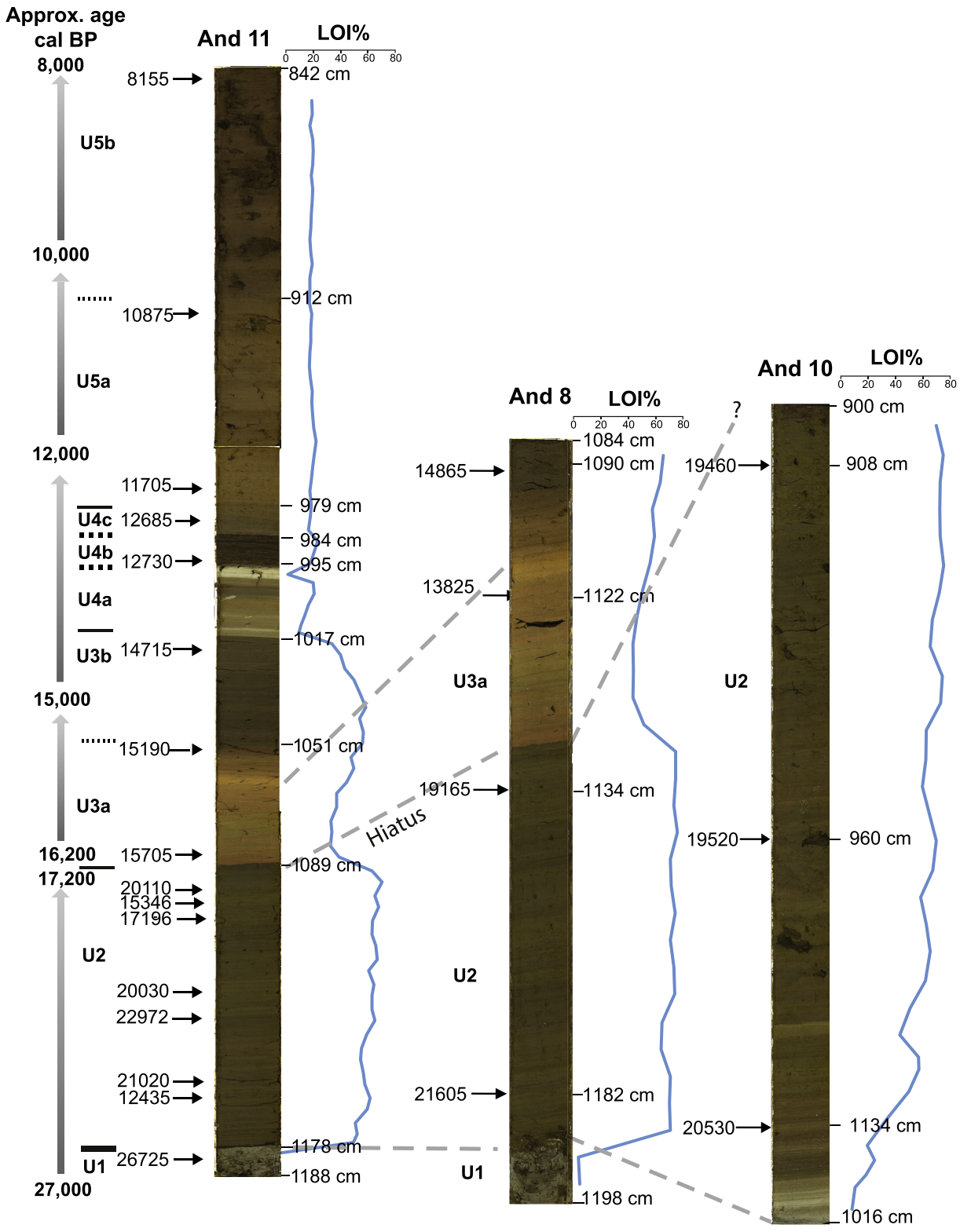

Fig. 3. Correlations between core And-11 (main core) and the shorter cores, And-8 and And-10. The alignment is based on lithological correlation and LOI. The dates given are median cal. years BP.

and thus often between samples for *sedaDNA*/pollen. If necessary, the samples were soaked in 10% sodium hydroxide (NaOH) to disperse organic material and/or sodium pyrophosphate ($Na_4P_2O_7 * 10H_2O$) to disaggregate clay particles. The macrofossils were retrieved by gently sieving the sample using a 250-μm mesh. The herbarium and the macrofossil reference collection at Tromsø Museum were used to aid identification.

3.6. sedaDNA, pollen and macrofossil data analyses

Initial diagrams were plotted in R studio version 1.2.5 using the rioja, vegan and ggplot2 packages. We explored zonation for three proxies using constrained incremental sum of squares (CONISS) as implemented in ggplot2 version 3.2.1. Final diagrams were constructed using Tilia v.2.6.1 (https://www.tiliait.com/).

3.7. Review of botanical records and reconstruction of minimum July temperature

We used an indicator-species approach to estimating minimum July temperature based on a compilation of all published palaeorecords of taxa from Andøya for the period 26.7–14.7 cal ka BP. The northern limits of vascular plants and vegetation types are closely linked to summer temperature (Karlsen and Elvebakk, 2003; Karlsen et al., 2005), and the Arctic is divided into bioclimatic zones representing mean July temperatures (Walker et al., 2005). We used the Pan-Arctic flora checklist (Elven et al., 2011) to assign species to the northernmost bioclimatic zones where they were (1) present or (2) frequent. If the palaeo-records were not determined to species level, the northernmost potential species in that taxon was used. Some taxa only identified to a higher taxonomic level were not classified, as ranges can be global (for example Poaceae). The choice of classification inevitably introduces bias, and our choices here lead to opposing biases regarding the kind of environment we reconstruct. First, at their northern limits most species have small population sizes and pollen production is typically low (Lamb and Edwards, 1988). Thus, a rare taxon has a low chance of occurring in palaeo records, whereas frequent species are more likely to be recorded (Schenk et al., 2020). Alternative (1) represents a conservative (cold) estimate of the minimum temperature (results given in Supplementary Table S2), whereas alternative (2) represents a mid-range estimate (results in main text) equivalent to "common northern distribution limit" (Schenk et al., 2020). Second, choice of the northernmost potential species in a group causes a strong bias towards more northerly, colder zones. For example, *Puccinellia* and *Ranunculus* occur in the polar desert zone although the majority of species in these genera do not reach the High Arctic (Elven et al., 2011); this classification in turn biases both alternatives towards colder environments.

4. Results

4.1. Bathymetry, chronology, lithostratigraphy and geochemical analysis

The updated bathymetry of lake Øvre Æråsen (Fig. 2) shows an irregular basin morphology with thick sediments across the shallow centre of the lake, and thin sediments in the deepest part. Given that the deepest sediments occur in a generally shallow area (an inversion of normal sedimentation pattern), it is unlikely that sediments have been deposited by erosion and more likely that either there has been erosional incision or that this has resulted from ice in the lake and a coarse boulder-dominated moraine. Whether a moraine or not, the altitude of the basin and its basal irregularity suggests disturbance of the basin in its early history. This is also suggested by the disturbed/tilted laminations in the basal sediments of Alm's (1993) core C.

Three new cores were taken and the most complete core (And-11, Fig. 3) is divided into 5 units, labelled U1 to U5, based on lithology (Table 2). The basal unit is a silty-sandy diamicton capped by a thin sand unit (U1), as is typical for basal sediments. Above this are laminated gyttjas (U2 olive green, U3a rusty brown, and U3b olive green), which are markedly different from typical glacial clays expected for this period. Then follows a unit of light olive grey to white laminated silts (U4a), a moss layer (U4b), and then above olive brown to dark olive brown gyttjas (U5a and U5b). The unit U4a (olive grey to white with laminated silts) is unusual, but it is not a simple carbonate as shown by no acid reaction (discussed further below). The moss layer above it is of *Warnstorfia fluitans* (U4b, 985–995 cm) is also interesting as this suggests erosion into the lake of the surface or the edge of an acidic mire. From the stratigraphy there is a clear hiatus at between U2 and U3a (1089 cm), and two other potential hiatuses at 1178 cm (in And11 but not And8), and possibly 995 cm (Fig. 3). The most parsimonious correlation based on the dates, LOI and the lithology is that the shorter core And-8 covers only part of U1-U3, while And-10 covers

Table 2
Lithological descriptions and modelled median age ranges. And-8 date in brackets inferred from And-11. Bacon dates in brackets extrapolated (1178 extrapolated from 1089 to 1156 using weighted mean).

Depth (cm)	Bacon k cal. BP	Unit	Description
And-11			
842–912	8.11–10.64	U5b	Dark olive brown gyttja
913–979	10.68–12.60	U5a	Olive brown silty gyttja
980–984	12.62–12.71	U4c	Dark brown silty gyttja
985–995	12.73–12.99	U4b	Moss layer (*Warnstorfia fluitans*).
996–1017	13.04–14.18	U4a	Bands of light olive grey to white silt. Lower boundary sharp
1018–1051	14.24–15.15	U3b	Laminated olive green gyttja. Lower boundary gradual.
1052–1089	15.17–16.18	U3a	Laminated rusty brown gyttja. Lower boundary sharp
	Hiatus (ca. 1 k years)		
1090–1178	17.23–23.25	U2	Laminated olive green gyttja. Lower boundary sharp
1179–1181*	23.31–23.45	U1	Silty-sandy diamicton. Sand layer at top (1 cm thick)
And-8			
1084–1093	*14.7–14.9*	U3b	Laminated olive green gyttja. Lower boundary gradual.
1093–1130	*14.9-(15.8)*	U3a	Laminated rusty brown gyttja. Lower boundary sharp
	Hiatus ?		
1130–1188	*19.0–21.9*	U2	Laminated olive green gyttja
1188–1191	*21.9–22.1*	U1/U2	Brown clay/gyttja
1191–1198	*22.1- ?*	U1	Silty diamicton, including pebbles
And-10			
900–954	*19.4–20.0*	U2	Coarse detritus gyttja
954–998	*20.0–20.5*	U2	Laminated gyttja
998–1010	*20.5–20.6*	U2	Laminated silty gyttja
1010–1016	*20.6- ?*	U1	Silt

only U2 (Fig. 3). Unless otherwise stated, the results are coherent for the three cores.

The 23 ^{14}C dates, which are all on identified plant macrofossils, range from ca. 8 cal ka BP to 26.7 cal ka BP (Table 1). Several of the dates acquired from small (<0.2 mg) samples have stratigraphically inverted ages (too old: Poz-77610; or anomalously young: Poz-104684). Although the small sample quantities affected the date precision there is no correlation between date precision and age (correlation coefficient 0.35) suggesting age is not a causative factor. We constructed an age-depth model for And-11 *with and without* specifying the upper two hiatuses (the lowest hiatus had only one date below making modelling impossible). When modelling the hiatus at 1089 cm depth in Bacon, 88% of the dates fell within the 95% range of the model, compared to 75% of the dates without the hiatus. The hiatus is estimated to cover the period ca. 17.2–16.2 cal ka BP. Based on the combined dates of And-11 and And-8 the age interval of unit U2 can be estimated as ca. 23.2–17.2 cal ka BP. The addition of another hiatus at 995 cm was found not to improve or significantly alter the model. Thus, the model including a single hiatus at 1089 cm was preferred (Fig. 4). The modelled basal range and median were similar for the models, both with one hiatus (21,880-26,780, median 23,446 cal ka BP) and without (21,828-26,732, median 23,366 yr BP). However, there are good reasons to assume that the basal date (Poz-77656, median 26.7 cal ka BP) is accurate as it is in accordance with two bulk dates obtained by Alm (1993; T-8029A and T-8029B: 27,068-25,282 cal yr BP and 26,069-25,541 cal yr BP (at 2σ)). Our date on moss suggests that, contrary to Vorren et al.'s (2015) opinion, Alm's pre-22.0 cal ka BP dates cannot be dismissed just because they were bulk dates based on gyttja samples. This strongly suggests that a lake existed and the basin was (partially) deglaciated in the later part of GS-3, from ca. 26.7 cal ka BP; the oldest sediments, however, have been disturbed.

Below the stratigraphically identified and modelled hiatus at 1089 cm, we see a scatter of dates based on moss fragments. This may be related to local reworking. Local reworking would still require a local terrestrial source, which implies a lack of glacial cover somewhere in the basin at an early date. The scattered ages, basal bathymetry, sediment depths and stratigraphic disturbance could indicate that the basin was partially covered by glacial ice from the cirque above it or possibly a palsa during GS3-GS2 (27.5–17.2 cal ka BP), both of which are possible given the location of the site adjacent to the postulated ice marginal limits (Vorren et al., 2015). However, on balance we accept the U1 and U2 dates as reflecting largely ice free conditions through the last of the Weichselian glacial expansions (MIS3-2) on three principal grounds:

1. All except three samples used terrestrial vascular plant fragments (mostly seeds) and mosses. The mosses dated were all terrestrial or *Warnstorfia fluitans* which although semi-aquatic (mires) is not submerged and takes up C from the atmosphere on acidic mires. Thus the mosses will not have a hard-water error and cannot have skewed the radiocarbon ages.
2. Due to the geology (entirely non-calcareous - amphibolites, hornblende and mica-gneisses) the lake is acidic and the high δ^{13}C in the gyttja is not due to carbonate but due to microparticulate guano (apatite and digestive derivatives/urea/lipids; see below), so the lake water would not have been high in calcium bicarbonate.
3. The dates agree with cosmogenic exposure dates, three of which are from the bird cliff (Store Æråsen), 270 m from the edge of the lake. These are 37 ka BP, 37 ka BP and 45 ka BP, and slightly further way (1.57 km) at Murdalen, 54 ka BP (Nesje et al., 2007). Dates are also in line with the whole reconstruction of the Andøya - Skånland glacial transect by Nesje et al. (2007).

Taken together, all these dates and the glacial reconstructions suggest that the north tip of Andøya was not ice-covered during the last glacial advance of the Weichselian.

Geochemical analyses (C, N, δ^{15}N, δ^{13}C and XRF) were carried out on the And-11 core (Fig. 5); LOI measurements were performed on all three cores (Fig. 3). The most striking feature is the exceptionally high organic content in these MIS2 sediments from ca. 23.2 cal ka BP onwards. The geochemical analyses reveal four trends (Fig. 5). First, the organic content and associated elements (LOI, C%, N%, C/N, δ^{13}C, δ^{15}N, S, Cl and Ca) reach high values in units U2 and U3 . Second, all values, with exception of C/N and δ^{13}C, show a distinct drop in the lower half of U3, i.e., U3a: LOI 60–70%, (Figs. 3 and 5), and C ~50%, (Fig. 5), but organic content values remain unusually high for MIS2 sediments. Third, S, Cl and Ca co-vary with the LOI and C%, with the exception of an increase in Ca in unit U5b and a contrasting trend in K, Ti and Fe. In U1 to U4, these elements are negatively correlated with the organic content, and they are interpreted as representing material eroded from the catchment. The fourth trend is in Si. This element is also negatively correlated with the organic content, but in contrast to K, Ti and Fe, it increases markedly in U5. This likely signifies erosion of base-depleted soils (Boyle, 2007). Low LOI, and high K, Ti and Fe in U3–U4, indicate mineral soil depletion, suggesting temperatures above 0 °C, at least seasonally, and some soil formation and erosion.

The unusually high δ^{13}C (−16 to −11) and δ^{15}N (18–22) values in units U2 and U3b (Fig. 6) indicate that the organic material is derived from a high trophic level. It is well outside the normal values for temperate, boreal or arctic lakes (Gąsiorowski and Sienkiewicz, 2013; Osburn et al., 2019; Thompson et al., 2018). Almost certainly, much of organic material is derived from sea-bird faeces (guano) and associated algal production, a suggestion originally made by Alm (1993). The C/N ratio is interpreted as reflecting preservation of this organic matter with moderately high N, prior to the Late Glacial and early Holocene.

4.2. Ancient DNA record

From 74 samples we obtained in total 22,888,821 raw reads, of which 1,707,668 reads of 45 sequences passed the initial filtering criteria of our pipeline (Supplementary Table S3). Two sequences matching *Vaccinium myrtillus/vitis-idaea* and three matching *Ranuculus reptans* were assumed homopolymer variants, and only the most frequent sequence was kept. Also two sequences matching pine (*Pinus*) were found. *Pinus1* was found in 19 samples (3.1% of the repeats of all samples) whereas *Pinus2* was only found in six PCR repeats at 894 cm depth in core And-11. The following taxa were found in negative controls after the filtering pipeline: spruce (*Picea*, one repeat in each of three negative controls from sampling and extraction), and one repeat of each of *Betula, Pinus1,* Poaceae and Brassicaceae. The frequency of PCR repeats of these taxa was lower in samples than in negative controls for *Picea* (0.83) and Brassicaceae (0.26), and these taxa were therefore excluded, whereas the frequency of *Pinus1* and *Betula* were 2.7 and 4.6 times higher in samples than in negative controls, respectively, and therefore kept in the dataset (Table S4). All 39 taxa, including negative controls, are presented in Supplementary Table S4, whereas the 37 assumed true positive taxa are included in Figs. 7 and 8. All taxa were found in core And-11. Cores And-8 and And-10 each contained eight taxa (Supplementary Table S4). The majority of the taxa were identified to a taxonomic level that allowed classification according to bioclimatic zones (Supplementary

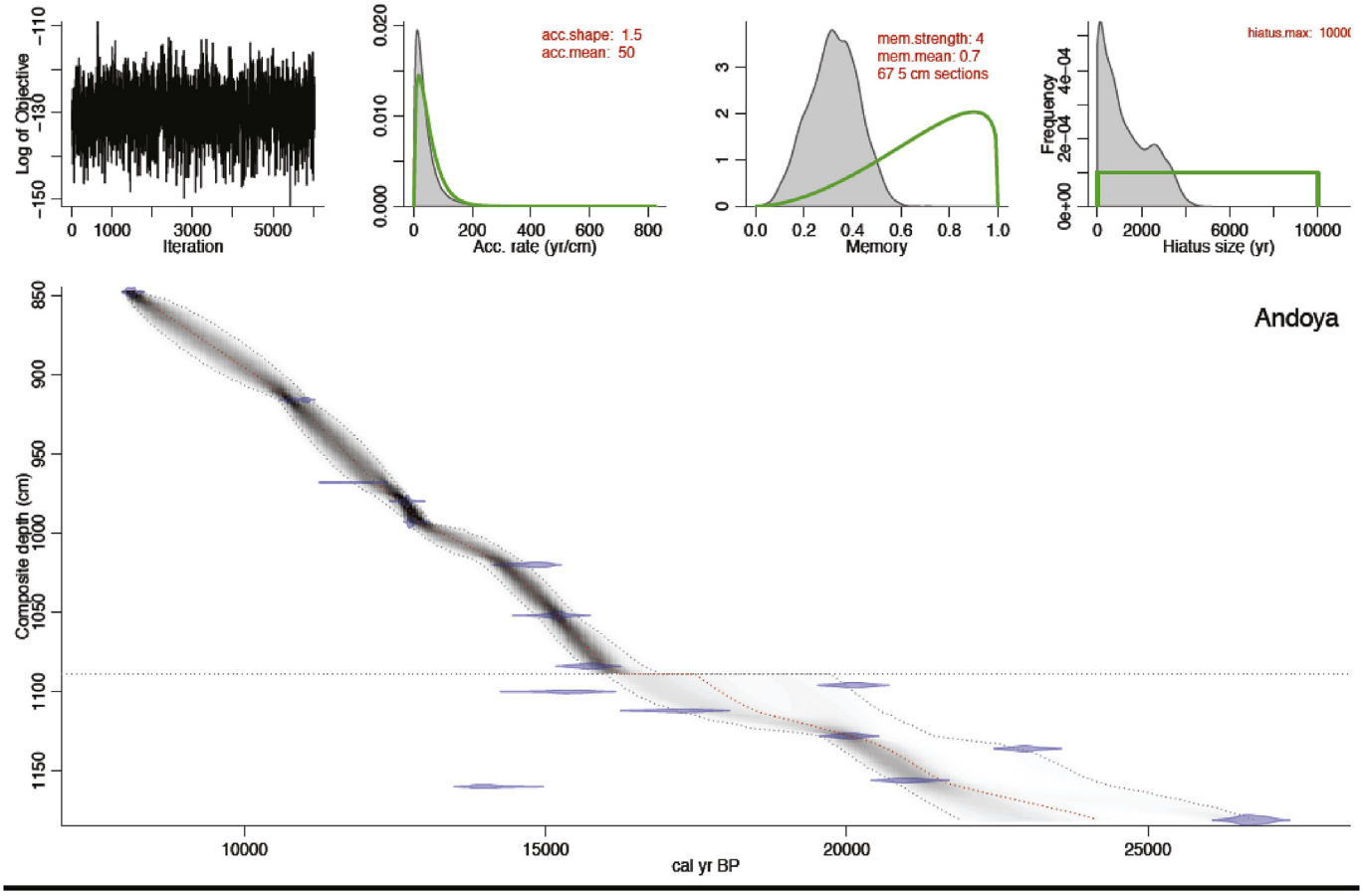

Fig. 4. Age-depth model for core And-11 from Øvre Æråsvatnet, Andøya, Norway. The calibrated 14C age ranges are shown in blue. The red lines show the statistically best model based on average of the mean, and the stippled lines show the 95% confidence interval. The horizontal stippled line shows hiatus at 1089 cm depth. (For interpretation of the references to colour in this figure legend, the reader is referred to the Web version of this article.)

Table S5).

Taxonomic diversity was generally low in samples older than 12.7 cal ka BP, with 0–5 taxa per sample, but it increased to 13–22 taxa in more recent samples. The highest read abundances were found for *Pinus, Ceratophyllum demersum, Myriophyllum alterniflorum,* Poaceae, and algae (*Nannochloropsis* spp.) (all > 90,000 reads). However, a more conservative estimate of DNA quantity is the number of PCR replicates, and here *Nannochloropsis gaditana* and *Nannochloropsis* sp. were by far the most dominant with 307 and 301 replicates, respectively, compared to 41 of *Caltha palustris,* 40 *Myriophyllum alterniflorum*, 39 Poaceae, and 37 PCR replicates of *Betula*.

4.3. Pollen record

In total, 60 pollen and spore types were identified in 19 samples (Supplementary Table S6) No pollen or spores were found in the basal diamicton; four samples in the basal zone (>14.2 cal ka BP) were essentially barren with dry-land pollen sums <5. The three youngest samples yielded >100 grains of pollen and spores. All total dry-land pollen spore concentration values were below 4000 grains per cm^3 except the two youngest, which had values of 8000 and 12,500 grains cm^3. Less than 5 taxa (including ferns and fern allies) occurred in the lower zone, but up to 29 taxa occur in samples in the youngest zone. Most frequent grains/spores were Pteropsida (monolete spores, total count 496), Poaceae (303), *Betula*-tree type (mainly in Holocene samples, 165), and *Gymnocarpium dryopteris* (also in Holocene samples, 120). The only consistent and relatively abundant pollen taxon prior to 14.2 cal ka BP was Poaceae. There was a clear increase in taxon richness from oldest to youngest sediments, whereas except for the two youngest samples, there was no clear pattern in concentration (Supplementary Table S6). In total, 46 of the 60 pollen and spore types could be classified to bioclimatic zones (Supplementary Table S5; Supplementary Fig. S1.

4.4. Macrofossil record

The 44 macrofossil samples included 503 records of 19 taxa/types of vascular plants, bryophytes, insect fragments, *Daphnia* ephippia and *Chara* oospores, with taxa mostly identified to species or genus level (raw counts in Supplementary Table S7). For the majority of samples, 0–3 taxa of vascular plants were found, with 4–6 taxa for the three youngest samples. Bryophytes were found in all samples (typically <50 fragments) and insect remains in most samples (typically >1000). Other abundant macrofossils were Poaceae (148 seeds), *Papaver* (110 seeds), and Brassicaceae (*Draba*-type; 15 seeds). There was a clear turnover in the macrofossil record from a dominance of *Papaver,* Poaceae and Brassicaceae to *Salix* and *Saxifraga* around 14.2 cal ka BP, and subsequently to *Betula* and aquatics from 10.5 cal ka BP onwards (Supplementary Fig. S2).

4.5. Combined vegetation zones

The CONISS analyses suggested five periods for each of *sed*aDNA,

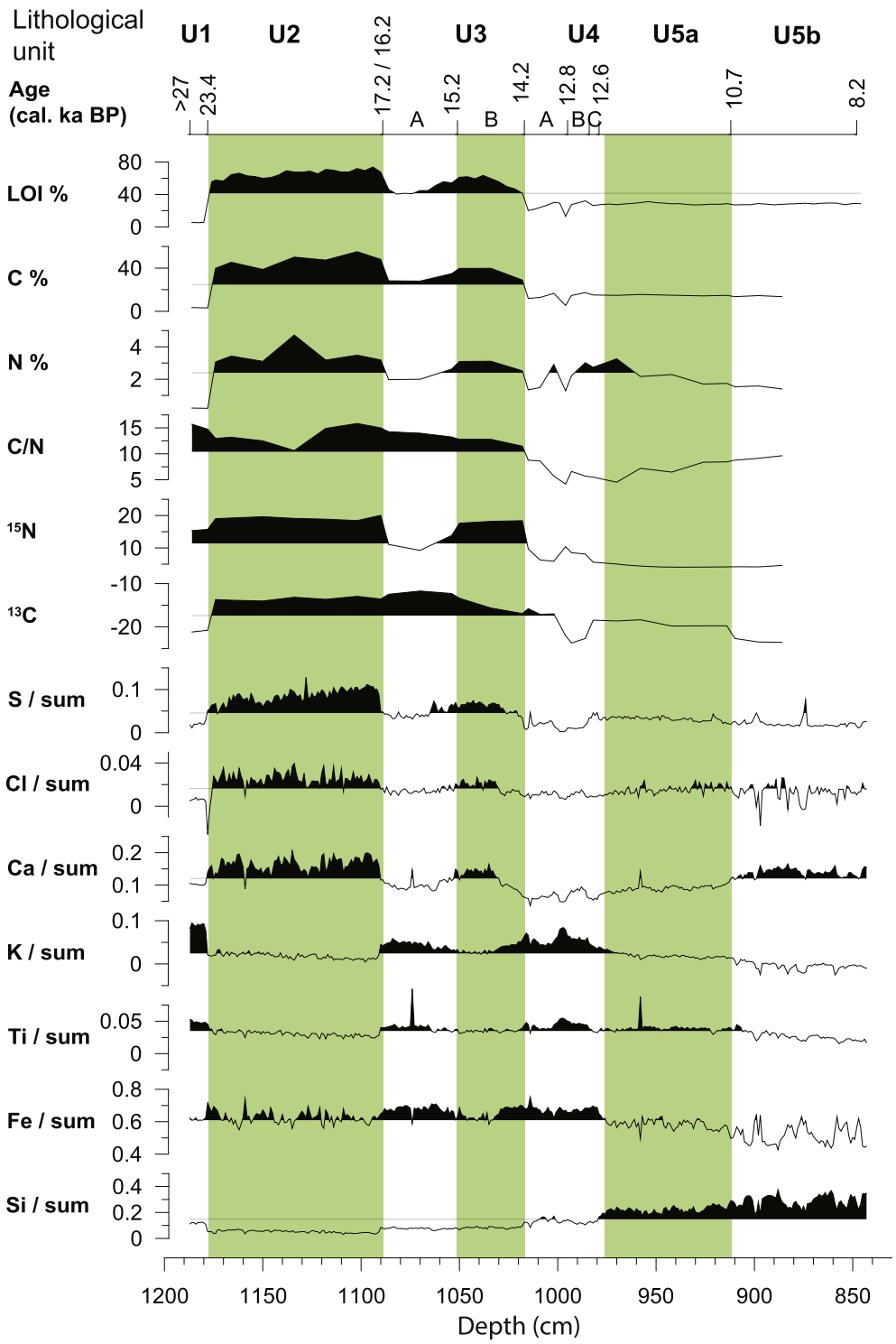

Fig. 5. Sediment properties of the core And-11 from Øvre Æråsvatnet, Andøya, Norway. Lithostratigraphic units U1-U5 are marked. The data are shown on a depth scale, with the age shown for unit boundaries. Selected elements of XRF analyses are shown as a ratio with Ti except Ti which is shown as ratio to the sum of all elements. Values above the mean are shown in black. The dates given are median cal. ka BP.

pollen and macrofossils, but zone boundaries differed in age/depth (Supplementary Fig. S3). The only boundary identified in all three proxies, and also in the lithology, was at ca. 1018 cm depth (14.2 cal ka BP, range 13.9–14.6 cal ka BP). This is close to what is generally seen as the end of GS-2.1a (14.7 cal ka BP, (Rasmussen et al., 2014), so we use this as a major boundary. Zonation before 14.2 cal BP is based on few taxa in each of the records and thus not robust. Therefore, we keep this as one zone. After 14.2 cal ka BP, there is a step-wise zonation with first a boundary in macrofossils around 12.8, pollen at 10.8 and 10.6, and then *seda*DNA at 9.6 cal ka BP (Fig. 7). Below, we discuss the two major zones and their minor zonation. Cores And-8 and And-10 are both within zone 1.

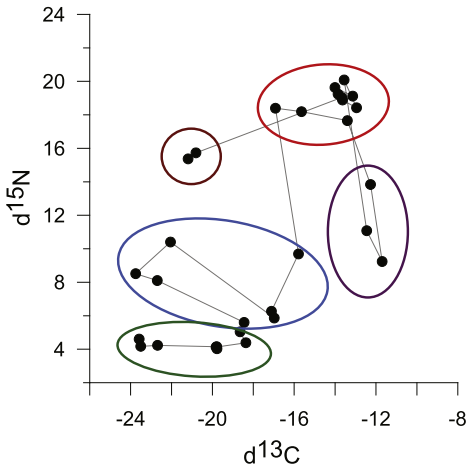

Fig. 6. A bi-plot of stable isotopes of nitrogen $\delta^{15}N$ and carbon $\delta^{13}C$ in core And-11, Øvre Æråsvatnet, Andøya, Norway. The lithological units U1-U5 are marked. Note that the age of the units spans the period 24 cal ka BP (U1) to 8 cal ka BP (U5). Stippled line indicate age from oldest (U1) to youngest (U6) sediments.

4.6. Zone 1: 24.0–14.2 cal ka BP (1182-1018 cm)

Taxon numbers per sample are low for all proxies (*seda*DNA 1–4, pollen 1–4, and macrofossils 2–6; Fig. 7). Of taxa present, most frequent are Poaceae, *Papaver* and Brassicaceae. Poaceae is a consistent taxon in all three proxies with relatively high concentrations of pollen and macrofossils. *Papaver* is recorded mostly as macrofossils (Fig. 7), occurring in all samples with up to 11 seeds per sample (Supplementary Table S7). Poaceae and *Papaver* are also present in And-8 and And-10 (Supplementary Tables S4). Brassicaceae (*Draba* type) occurs in ~50% of pollen and macrofossil samples, whereas the one *seda*DNA record was filtered out (see above and Supplementary Table S4). While ubiquitous as macrofossils, *seda*DNA of bryophytes were not found in this zone. This may be due to "swamping" of the *seda*DNA by algae (*Nannochloropsis* sp., *N. gaditana*, and for one sample in And-8 also *N. granulata*).

Other forbs present as *seda*DNA are Apiaceae (most likely *Angelica archangelica*), found in all three cores (few PCR repeats) and *Potamogeton* cf. *grammineus/alpinus*. Also present as single records are *Aster* sect. *Aster* (pollen), *Potentilla* (pollen), and cf. *Alchemilla alpina* (macrofossil; Fig. 7, Supplementary Tables S4, S6, and S7). Of the woody taxa, *Pinus seda*DNA occurs in three And-11 samples (Fig. 8) and in one and two samples in And-8 and And-10, respectively (Supplementary Table S4). It was also found as single grains in each of two pollen samples (Supplementary Table S6), but not the same ones as the *seda*DNA (Fig. 7). *Salix* occurs in a single *seda*DNA sample (And-10, Supplementary Table S4) and as a single pollen grain (Fig. 7) but not as macrofossils (Supplementary Table S7). Other woody taxa recorded were *Betula*-tree type (single grain), *Quercus* (single grain in two samples), and *Sorbus seda*DNA samples (one sample at about 14.4 cal ka BP).

Insect fragments occur in all except the lowermost samples, increasing in abundance from around 15.5 cal ka BP. From ca. 15.0 cal ka BP, *Daphnia* ephippia rapidly become abundant (Fig. 7). Although generally eurythermal, most *Daphnia* species require a minimum water temperature of 10 °C (Clare, 2018). A bone attributed to little auk (*Alle alle*) was found at 1178 cm in And-8 (ca. 22.2–21.0 cal ka BP), and a similar bird bone was found at 1004 cm in And-10. The number of *Nannochloropsis* repeats drops between 16.2 and 15.2 cal ka BP, which is also when the sediments show a drop in LOI, C and N isotopes (Figs. 5 and 6).

4.7. Zone 2 sedaDNA, pollen and macrofossils 14.2–8.2 cal ka BP (1018- 850 cm)

Pinus is scattered in the *seda*DNA and pollen records, sometimes present in the same samples (Fig. 8a). *Salix* macrofossils appear from around 14.2 cal ka BP, followed by *Salix* pollen and *seda*DNA (Fig. 8a). There are no samples analysed for pollen and macrofossils in the youngest sediments, but *Salix* remains frequent in the

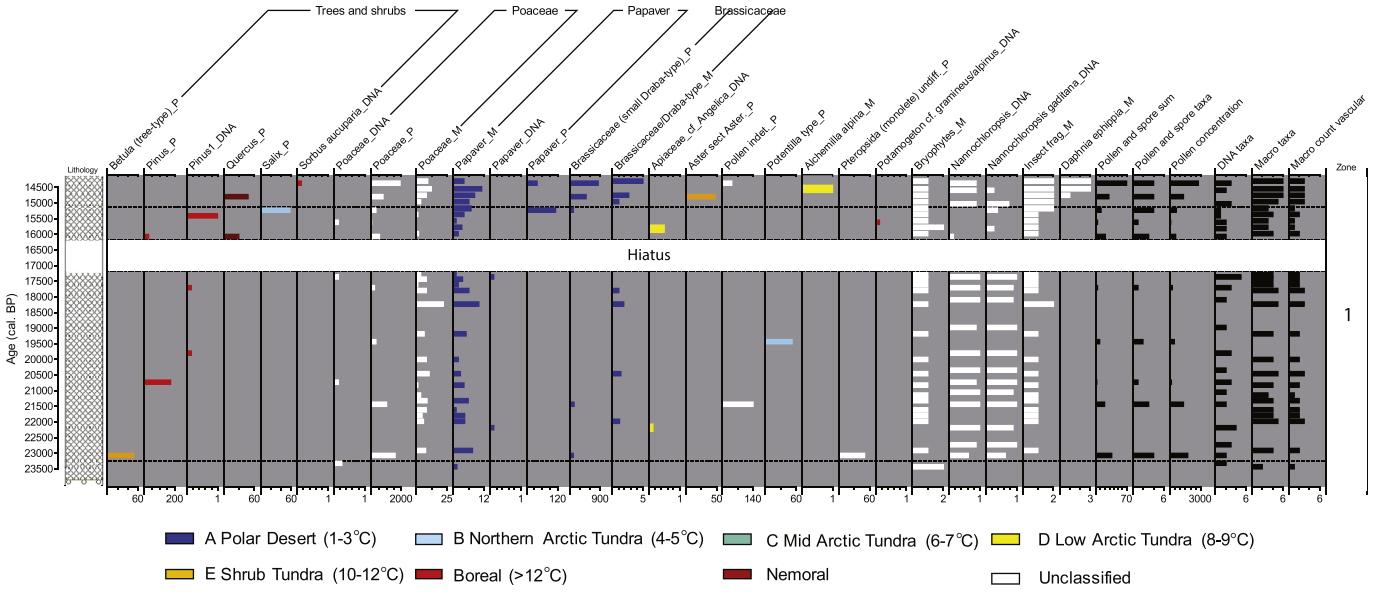

Fig. 7. Ancient sediment DNA (*seda*DNA), pollen and macrofossils recorded in core And-11 from Øvre Æråsvatnet (Andøya, Norway) from 23.5 cal ka BP to 14.2 cal ka BP. *Seda*DNA data are presented as proportion out of 8 PCR repeats, macrofossils as seeds per 50 cm^{-3} and pollen and spores as grains per cm^3. Note that the x-axes are scaled according to occurrence within each taxa and proxy; *seda*DNA data are all scaled to 1. Colour codes are according to northernmost bioclimatic subzone where the taxa is frequent (see methods). The stippled lines shows lithological units (see Fig. 3). (For interpretation of the references to colour in this figure legend, the reader is referred to the Web version of this article.)

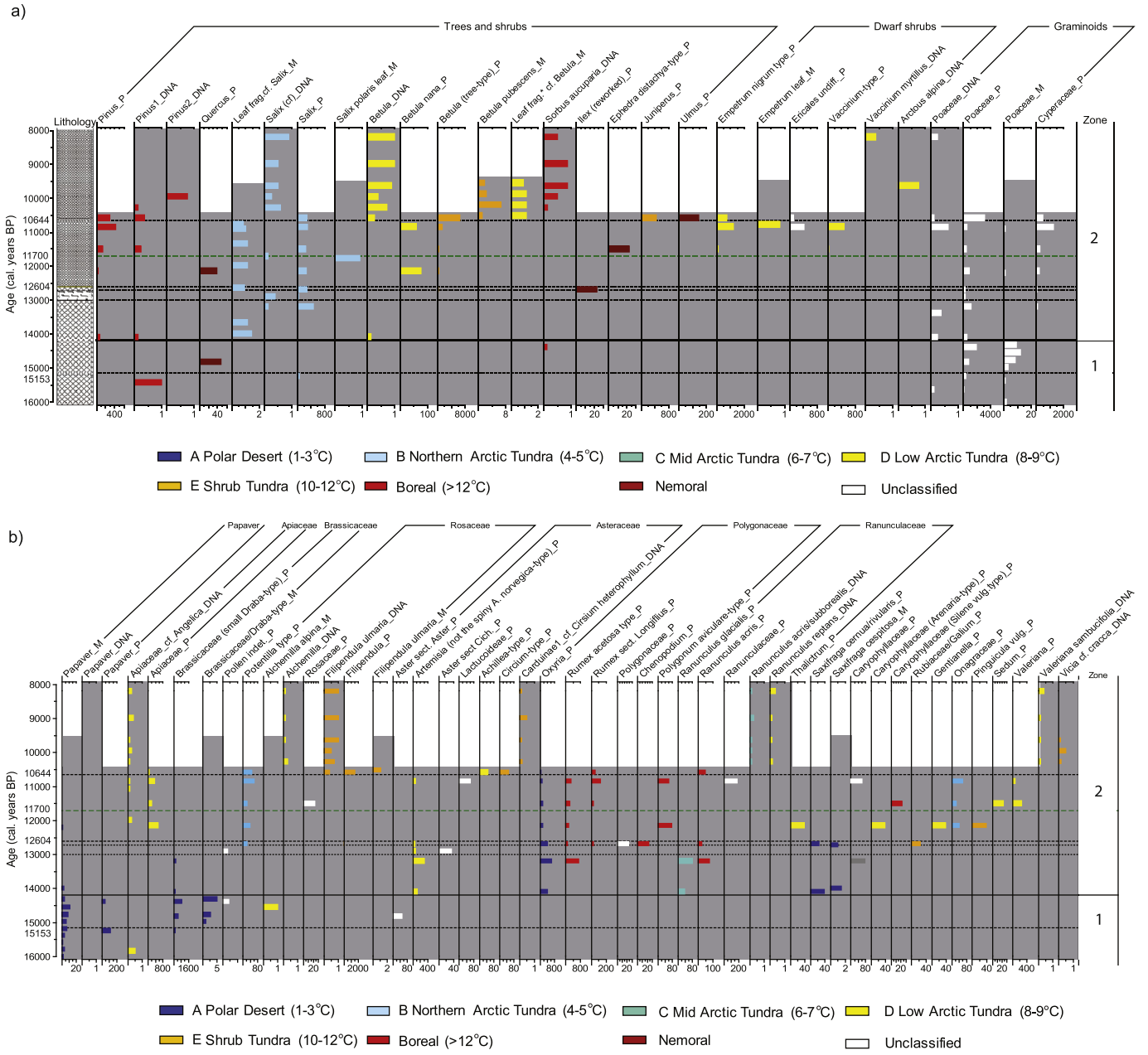

Fig. 8. Ancient sediment DNA (*seda*DNA), pollen and macrofossils recorded in core And-11 from Øvre Æråsvatnet (Andøya, Norway) from 16 cal ka BP to 8 cal ka BP. *Seda*DNA data are presented as proportion out of 8 PCR repeats, macrofossils as seeds per 50 cm^{-3} and pollen and spores as grains per cm^3. Note that the x-axes are scaled according to occurrence within each taxa and proxy; *seda*DNA data are all scaled to 1. Colour codes indicate northernmost bioclimatic subzone where the taxa is frequent (see methods). The stippled lines shows lithological units (see Fig. 3). Note that the youngest pollen and macrofossil counts were 10570 and 9540 cal ka BP, respectively. a) Trees, shrubs, dwarf shrubs and graminoids, b) forbs, and c) bryophytes, club mosses, horsetails, ferns, aquatic, algae, and others. (For interpretation of the references to colour in this figure legend, the reader is referred to the Web version of this article.)

*seda*DNA record. Poaceae is present as *seda*DNA and pollen, but it almost disappears as a macrofossil (only single seeds in two samples after 14.2 cal ka BP). *Papaver* and Brassicaceae (*Draba* type) almost disappear, but new forbs appear, e.g. *Artemisia, Oxyria, Ranunculus glacialis* (all as pollen), and *Saxifraga* spp. (pollen and macrofossils) (Fig. 8b). *Salix* was not identified to species, but given the other species in the assemblage, it likely represents dwarf shrubs such as *S. herbacea, S. polaris*, and/or *S. reticulata*. *Salix* is rare in bioclimatic zone A, the Polar Desert Zone (Walker et al., 2005), so conditions must have been warmer than that. Except for pine, no boreal species are recorded until 13.2 cal ka BP, suggesting an arctic tundra until then.

From around 13.2 cal ka BP, the pollen spectra include a few boreal forbs, such as *Rumex* and *Ranuculus acris*, and *Artemisia* is still present (common in low-arctic tundra but pollen potentially extra-regional, 1–4 grains per sample, Table S6) possibly suggesting an increase in temperature. In three samples dating to 12.9–12.7 cal ka BP there is a short-lived appearance of several *seda*DNA bryophyte taxa, reflected also in higher abundance of bryophyte macrofossils (Fig. 8c) and a bryophyte band in the lithology (U4b;

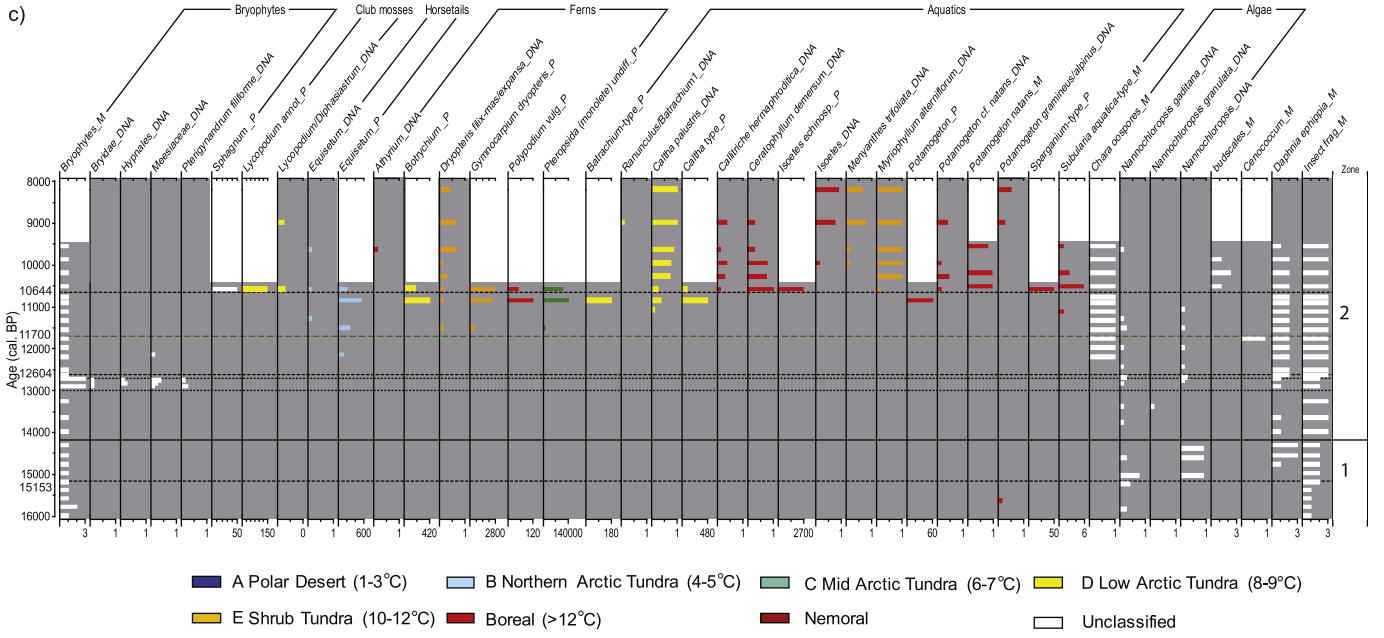

Fig. 8. (*continued*).

Fig. 3). Just above that, in U4a, there is a mixture of cold-adapted species such as *Potentilla, Oxyria*, and *Saxifraga* and boreal species such as *Rumex, Chenopodium* and *Galium*.

Soon after, at around 12.0 cal ka BP, Apiaceae re-appears along with new taxa that have distributions north to the Low Arctic Tundra Zone: *Thalictrum,* Caryophyllaceae (*Arenaria* type), *Betula nana* and *Gentianella.* These changes suggest a transition to Low Arctic Tundra Zone or Shrub Tundra Zone, although we note that dwarf shrubs do not appear until around 11.5 cal ka BP (scattered pollen) and are more common from 10.8 cal ka BP. *Nannochloropsis* taxa show a clear drop from 14.2 cal ka BP, with only scattered occurrences subsequently, whereas *Chara* oospores occur in every macrofossil sample from 12.2 cal ka BP upwards, suggesting increasing water temperatures and some leaching of minerals from the bedrock.

The onset of the Holocene (11.7 cal ka BP, green line in Fig. 8) is not very pronounced in the record as only a few new taxa occur (e.g. *Valeriana, Sedum,* scattered ferns) and diversity is still low in all three proxies. The largest increase in number of taxa is at around 10.8–10.6 cal ka BP with a sudden jump from around 20 to 28–29 taxa in the pollen record, from 3 to 4 to 13–18 taxa in the *seda*DNA record, and from 1 to 2 to 5–6 taxa in the macrofossil record (Supplementary Tables S4, S6-S7). *Betula* becomes common in all three proxies, with pollen attributed to *Betula* tree type and macrofossils identified as *B. pubescens*.. At the same time, *Filipendula ulmaria* appears in all three proxies, and ferns are abundant. The assemblage suggests a tall-herb birch forest. Aquatic floristic diversity increases with the appearance of *Caltha palustris, Isoetes, Menyanthes trifoliata, Myriophyllum alterniflorum, Potamogeton* spp., *Sparganium* and *Subularia aquatica* (Fig. 8c). *Pinus* is found scattered in both pollen and *seda*DNA, with the highest concentration around 12.1 to 10.0 cal ka BP (Fig. 8a). *Picea* is also found in a total of 7 of the 23 *seda*DNA samples in the period after 14.2 cal ka BP (Supplementary Table S4), but note that we suspect records of *Picea* to be false positives.

4.8. Synthesis of Andøya plant and animal record >14.7 cal ka BP

In total, 94 vascular plant taxa have been recorded from pollen (77 taxa), macrofossil (19) and aDNA (9) studies (Supplementary Table S2, S8). A megafossil of *Betula pubescens* was recorded from nearby Stavdalen (ca. 20.4 cal ka BP, Kullman, 2006) . The most abundant taxa, both in this and previous studies, are Poaceae, Brassicaceae and *Papaver*. Poaceae may potentially include *Bromus, Festuca, Phippsia algida* and *Puccinellia.* Brassicaceae may include *Braya*-type, *Cardamine nymannii, Cochlearia,* and *Draba*-type. Vorren (1978) notes that the pollen indicates two different taxa of *Papaver*, whereas Alm and Birks (1991) note that the variation within *Papaver* seeds falls within *P. radicatum* s.lat. While over one third of recorded taxa have a northern limit in Shrub Tundra Zone (July temperatures 10–12 °C) or more southern zones, the majority of these are found only as occasional pollen types that may derive from long-distance transport. A few of these, however, occur as macrofossils and/or in *seda*DNA (Table 3, Supplementary Table S2) and are likely to have grown *in-situ*.

Further taxa identified during the LGM and early late glacial include caddisflies and chironomids (23.5 cal ka BP, Øvre Ærå-svatnet, (Solem and Alm, 1994), Nedre Ærsåvatn – mainly 16.9 cal ka BP onwards (Alm and Willassen, 1993) and Endletvatn, 22–14.7 cal ka BP (Elverland and Alm, 2012), and the beetle *Dier-nerella filum* (ca. 18-17 and 15.5 cal ka BP, Endletvatn, Elverland and Alm, 2012). The records of taxa indicating warmer conditions largely coincide with periods of higher pollen and macrofossil concentrations (Alm, 1993; Parducci et al., 2012a). The caddisfly *Apatania zonella* is a continental species with a distribution extending east of the LGM limit to the Urals (Fauna Europaea), although it could have survived the LGM at Andøya (Solem and Alm, 1994). *Dienerella* is cosmopolitan genus, with its current Norwegian distribution restricted to a few sites in the south and one in the north. It is associated with rotting wood and musty fruit bodies of soil fungi, but it is also found in arctic tundra (Elverland and Alm, 2012, https://www.artsdatabanken.no/). Furthermore, there are records of little auk dated ca. 20-15 cal ka BP (Alm and

Table 3
Thermophilous and other selected taxa of MIS2 age. July temperature of the bioclimatic zone where the taxon is found as frequent (Temp.1) or rare/scattered (Temp.2) today. *Indirectly dated to the period 21.4–20.1 ka cal. BP by Vorren et al. (2013). Uncertain temperatures due to uncertain taxon identifications are in brackets.

Taxa	Date	Temp.1	Temp2	Type	Site	Reference
Andøya thermomer 1, ca. 24–23 ka cal. BP (IS2, Andøya interstadial)						
Sphagnum leaves	ca. 25	8–9		macrofossil	Øvre Æråsvatnet	Alm (1993), unpub. data
Rumex acetosa	23.2	>12	10–12	macrofossil	Nedre Æråsvatnet	Alm and Birks (1991)
Saxifraga cespitosa	23.2	1–3	1–3	macrofossil	Nedre Æråsvatnet	Alm and Birks (1991)
Andøya thermomer 2, ca. 22–20 ka cal. BP (LGM)						
Chrysosplenium	22.0	6–7	4–5	macrofossil	Nedre Æråsvatnet	Alm and Birks (1991)
Pinus	22.0	(>12)	(10–12)	*seda*DNA	Endletvatn	Parducci et al. (2012a, b)
Brya-type (*B. linearis*)	≤21.8	(8)	(6–7)	macrofossil	Endletvatn	Elverland and Alm (2012)
Apiaceae	≤21.8	8–9	8–9	*seda*DNA	Øvre Æråsvatnet	Present
Apioideae (Apiaceae)	≤21.8	8–9	8–9	*seda*DNA	Endletvatn	Parducci et al. (2012a, b)
Sphagnum papillosum	ca. 21	8		macrofossil	Endletvatn	Vorren (1978)
Mustela erminea	ca. 20.8*	3		vertebrae	Endletevatn	Fjellberg (1978)
Betula pubescens	20.4	10–12	10–12	megafossil	Stavedalen	Kullman (2006)
Urtica dioica	19.8	>12	10–12	macrofossil	Endletvatn	Parducci et al. (2012a, b)
Andøya thermomer 3, ca. 19–18 ka cal. BP (LGM)						
Pinus	19.2	(>12)	(10–12)	*seda*DNA	Endletvatn	Parducci et al. (2012a, b)
Sphagnum papillosum	ca. 18	8		macrofossil	Endletvatn	Vorren (1978)
Picea abies	17.7	(>12)	(10–12)	*seda*DNA	Endletvatn	Parducci et al. (2012a, b)
Andøya thermomer 4, ca. 15 ka cal. BP (pre-Bølling warming)						
Sphagnum papillosum	ca. 15	8		macrofossil	Endletvatn	Vorren (1978)
S. cf. *platyphyllum*	ca. 15	8		macrofossil	Endletvatn	Vorren (1978)
Scorpidium scorpioides	ca. 15	3		macrofossil	Endletvatn	Vorren (1978)
cf. *Alchemilla alpina*	14.9	(8–9)	(8–9)	macrofossil	Øvre Æråsvatnet	Present

Elverland, 2012), eider duck (*Somateria* sp.) ca. 17.3 cal ka BP (Vorren et al., 1988), and stoat (*Mustela erminea*) ca. 20.1–21.4 cal ka BP (Endletvatn, (Fjellberg, 1978), re-dated by (Vorren et al., 2013).

5. Discussion

5.1. The LGM and glaciation of Andøya

Our new date >26 cal ka BP strongly supports the interpretation that the northern tip of Andøya including Øvre Æråsvannet was ice-free from ca. 26 cal ka BP. The earliest period of sedimentation, corresponding to the later part of GS-3, is disturbed, probably due to ice and the lake's location at the glacial margin. This finding aligns with three cosmogenic dates from the adjacent ridge, Store Æråsen (105 m a.s.l., 36–45 cal ka BP, Nesje et al., 2007, Fig. 1). Vorren et al. (2013) cite the cosmogenic data; they argue that the possibility of non-erosive, cold-based glacial ice cannot be excluded. However, our new data indicate an open lake surrounded by vegetation with a nearby bird cliff. Vorren et al. (2013) also regard the earlier pre-20 cal ka BP dates of Alm (1993) as possibly reflecting reworking. Given our new radiocarbon dates, seven of which pre-date 20 cal ka BP and all of which are based on macrofossils, reworking also seems unlikely. The complex bathymetry combined with disturbance of the basal sediments in Øvre Æråsvatnet prior to 16 cal ka BP suggest ice melt within the lake, as has been observed on the floor of glaciated lakes in southern Norway (Eilertsen et al., 2016) or paraglacial disturbance (Ballantyne, 2002). A very similar pattern of scattered early dates has been observed further north at Hammerfest (Birks et al., 2012b). Our dates constrain the ice at the LGM on the northern tip of Andøya to a brief period after the Ålesund Interstadial (38-35 cal ka BP; (Mangerud et al., 1981) to 26 cal ka BP. Alternatively, as suggested by (Mangerud, 2003), an unglaciated refugium that included Røyken and adjacent peaks on northern Andøya persisted throughout the last glacial cycle.

This also has implications for the local glacial sequence. Either the outermost Egga I moraine is earlier than ca. 26 cal ka BP, as originally argued by Vorren and Plassen (2002), or it represents a terminal moraine of a glacier in Andfjorden, the surface of which was just below Øvre Æråsvatnet. This is possible, as the Egga I moraine lies at −240 to −250 m b.s.l. and cannot be linked to an outer moraine further to the south, due to the presence of the Andøya canyon. However, it also follows that ice depositing Egga 2 cannot have covered the lake, and the only correlative moraines on the tip of Andøya (Kjølhaug, Endleten, and off shore Bleik) are all to the east and below Øvre Æråsvatnet (Fig. 1). It therefore appears that during the LGM, a very small area of Andøya, including Øvre Æråsvatnet, was an ice-free area bounded to the north by ocean (ice or water depending on season), to the east by the edge of the ice sheet, and protected to the south and west by mountains.

Given the finds in the Sunnmøre caves of little auk, other seabirds, fox and reindeer (Larsen et al., 1987), the data now available suggest that periodically an ice-free corridor existed along the outer islands of Norway, with most areas being overrun during the LGM after 26 cal ka BP, except a small part of northern Andøya. Both the proximity of the continental shelf edge, and our data suggest that a large sea bird population was present; this was possibly favoured by a local polynya, as has been suggested for an apparent MIS 2 ice-free area off Svalbard (van der Bilt and Lane, 2019).

5.2. Does DNA of pine and spruce derive from locally growing trees?

As in the study of nearby lake Endletvatn (Parducci et al., 2012b), we recorded DNA of pine and spruce. For the conifer DNA in Endletvatn, local growth was suggested, but alternative sources such as driftwood, reworked older material, DNA leaching, or a pollen origin were also discussed (Birks et al., 2012a; Parducci et al., 2012a, 2012b). Later studies indicate that DNA leaching is not a problem (Clarke et al., 2019; Sjögren et al., 2017). This is supported by the Øvre Æråsvatnet data, where virtually none of the many taxa observed in Holocene levels (Fig. 8) was recorded in samples older than 14.2 cal ka BP (Fig. 7). Similarly, pollen is an unlikely source of chloroplast *seda*DNA (Niemeyer et al., 2017; Parducci et al., 2017; Sjögren et al., 2017), but there is less empirical evidence showing this for gymnosperms, which have paternally inherited chloroplasts. As only a few pine pollen grains were found, and these occurred in *seda*DNA samples in which no pine pollen was identified, pollen is not a likely source of pine and spruce DNA. The

likelihood of driftwood is low at Øvre Æråsvatnet, as it sits above the local marine limit. Furthermore, if driftwood were a source of *seda*DNA, we would expect to see a higher frequency of conifer DNA around 20.5 cal ka BP, when the nearby Endletvatn was transgressed by sea for a short period (Vorren et al., 1988, 2013). In line with previous interpretation (Alm, 1993), our new dates and palaeo-record do not indicate any signs of reworked pre-LGM material. Thus, of all the suggested sources, we think we can rule out driftwood, pollen, leaching and reworked material. This leaves contamination or local growth as explanations.

Previously, contamination was not thought to be a source of the *seda*DNA because the result had been repeated in two sediment cores and three independent laboratories (Parducci et al., 2012a, 2012b). Methodology has advanced, and we have improved all parts of the methodology (extraction protocol, negative controls at all steps, running eight rather than one PCR, unique tagging to minimize tag jumps, sequencing, and bioinformatics). Nevertheless, for low-frequency sequences, it is often impossible to distinguish between true and false positives (Alsos et al., 2018; Ficetola et al., 2015; Zinger et al., 2019). When comparing modern *seda*DNA with local vegetation, a trade-off exists between retaining the true positive (i.e., true, according to the vegetation surveys) and removal of the false positives. In a recent such study, strict cut-off levels that removed the majority of false positives also removed 33% of the true positives (Alsos et al., 2018).

For ancient DNA studies, the issue of true and false positives is more challenging as independent proxies are needed for their identification. In other studies, scattered *seda*DNA records have been confirmed by macrofossils, for example, *Arabis alpina* in Svalbard (Alsos et al., 2016). We tried authentication of ancient DNA via ancient damage patterns, but shotgun sequencing of two samples from Lake Øvre Æråsvatnet did not identify sufficient pine and spruce for ancient DNA damage pattern analysis (Lammers et al., 2020).

Pine and spruce DNA are especially challenging, as they, like common food plants, can potentially be part of background contamination, due to the presence of wood or paper labels where the reagents are produced (Boessenkool et al., 2014; Clarke et al., 2018). In our laboratory at Tromsø Museum, pine and spruce were detected in 1.62% (SD = 1.08, range 0–2.50%) and 1.99% (SD = 2.52, range 0–6.25), respectively, of the negative control PCR repeats (n = 1360 PCR repeats of 170 negative control samples), for samples processed during the same period as this study. Thus, the frequency of pine (3.3%) is marginally above the range of background contamination in our lab, whereas the frequency of spruce (3.1%) in the three Øvre Æråsvannet samples is within that range. It is possible that even low frequencies of conifer DNA may represent true positives. Recently identified *seda*DNA in samples from the Polar Urals (ca. 21.0 and 18.0 cal ka BP; (Clarke et al., 2019) aligns with finds of two *Picea abies* stomata dated to ca. 20.4 and 18.8 cal ka BP (Anne Bjune pers. comm. 2019). Nevertheless, as the pine and spruce DNA record of Øvre Æråsvatn were not confirmed by independent proxies, and as they are within or only marginally above the background contamination, we cannot conclude anything about local presence.

As for the spruce DNA record dated to 10.3–6.3 cal ka BP at Lake Rundtjørna, about 700 km further south (Parducci et al., 2012b), no new samples have been analysed from that region. As that study was focused on sediments that were considerably younger and closer in age to finds of megafossils in that region, there is currently no strong reason to reject the Rundtjørna spruce record.

5.3. The LGM and late glacial environment: a productivity hotspot?

The stable $\delta^{13}C/\delta^{15}N$ values from the lower units of And-11 (U2-U3b) are highly unusual for lake sediments and indicate a marine nutrient source and high trophic level. Little auk bones were found within the enriched sediments and also at Endletvatn (ca. 20-15 cal ka BP, Elverland and Alm, 2012), along with bones of eider duck (*Somateria* sp.) at ca. 17.3 cal ka BP (Vorren et al., 1988). The presence of ground-nesting birds is further supported by the discovery of bones of stoat (*Mustela erminea*) at Endletvatn in the interval 20.1–21.4 cal ka BP (Fjellberg, 1978, re-dated by Vorren et al., 2013). Profundal sediments from high-arctic lakes in NW Greenland affected by marine-derived nutrients from little auk colonies show a 10-fold increase in $\delta^{15}N$ values over other sites ($\delta^{15}N$ 20.7 ± 2.4 SD), together with values for aquatic moss of 17.3 ± 5.8 and benthic algae of 17.9 ± 8.8 (González-Bergonzoni et al., 2017); these are similar to the $\delta^{15}N$ values of unit U2 (23.2–17.2 cal ka BP.) and unit U3b (15.1–14.2 cal ka BP) at Øvre Æråsvatnet. The Andøya data strongly suggest presence of a substantial sea-bird colony, and it is likely the lake and its surroundings were heavily manured. Furthermore, the bryophyte *Syntrichia ruralis* prefers alkaline substrates and high nitrogen (Vorren et al., 2013, http://www.arcticatlas.org). It has been estimated that marine-derived nutrients from little auk colonies underpin more than 85% of terrestrial and aquatic biomass in affected areas (González-Bergonzoni et al., 2017). Such an increase in nutrient input would also greatly increase primary production, which fits with the unusually high organic content of the sediments for LGM and the dominance of the algae *Nannochloropsis* in the *seda*DNA record.

Our *seda*DNA, pollen and macrofossil record for the period 24–14.2 cal ka BP is relatively species-poor and dominated by very few taxa (Poaceae, Brassicaceae, and *Papaver*). Neither fossil pollen assemblages nor modern plant communities provide close analogues. The modern Arctic vegetation unit B1 (cryptogam-herb barren) of the Circumpolar Arctic vegetation map (Walker et al., 2005) is most similar, but fossil pollen, *seda*DNA and macrofossil records from the northernmost bioclimatic zones show a diversity in the flora rather than dominance by these three taxa (e.g. Alsos et al., 2016; Bennike, 1999; Bennike and Hedenäs, 1995; Birks, 1991; Hyvärinen, 1970). In our records, the high abundance of *Papaver* probably reflects a lack of competition (Modin, 2016) combined with the availability of favourable habitats, such as screes and gravel bed channels. In the modern Arctic, high values of Brassicaceae pollen are found in association with bird-manured soils (Rozema et al., 2006; van der Knaap, 1988). Given convincing evidence of a bird colony, bird–manured arctic vegetation, combined with disturbed ground habitats in other parts of the catchment, maybe the best descriptor to the LGM vegetation on Andøya.

The four phases of warmer temperature that have been observed in previous studies (Table 3, Alm, 1993; Alm and Birks, 1991; Elverland and Alm, 2012; Vorren et al., 1988, 2013), are not pronounced in the current record (Fig. 7). The lack of signal may relate to the unusual situation of the lake. The high percentages of algal *seda*DNA likely masked DNA of terrestrial taxa, as has been inferred from modern studies (Alsos et al., 2018). Pollen abundance in many LGM records was so low that extended counting would have yielded little information; pollen is extremely diluted by the high lacustrine productivity, and this problem applies to macrofossil counts also.

If we assume that the DNA records of *Picea* and *Pinus* are due to contamination and that pollen of *Betula* and *Quercus* is exotic, the only thermophilic species prior to 16 cal ka BP in the current record is Apiaceae. The sequence has 100% match to several species of *Angelica* and *Heracleum*, as well as *Conioselinum tataricum* and *Podistera macounii*. Based on current biogeography and northern limits of these taxa, the sequence most likely represents *Angelica*

archangelica, a species that can reach high abundances along bird cliffs today (Grønlie, 1948) and that has its current northernmost limit in the Low Arctic Tundra (8–9 °C July temperature) where it is frequent (Elven et al., 2011). The occurrence of Apiaceae is within the Andøya thermomer 2 (22–20 cal ka BP; Table 3), concurrent with the Endletvatn *sedaDNA* record (Parducci et al., 2012b), and within the period of high nitrogen and carbon isotope values (Figs. 5 and 6). This interval provides the strongest evidence of climate amelioration: the occurrence of several macrofossils with thermal limit at around 8 °C (Elverland and Alm, 2012; Kullman, 2006; Vorren, 1978) plus *Urtica dioica,* which is rare in the Shrub Tundra (10–12 °C) and common in the Boreal Zone (Elven et al., 2011; Parducci et al., 2012b).

A few more thermophilic taxa occur in our record from 15.8 to 14.2 cal ka BP. We note that these are species that are either common beneath bird cliffs (e.g. *Alchemilla alpina*, *Angelica archangelica*) and/or easily dispersed by birds (*Potamogeton*, *Sorbus aucuparia*). They occur in lithological unit U3b, which is rich in nitrogen and carbon (Figs. 4 and 5). Both *Sorbus aucuparia* and *Potamogeton* are common north to the boreal zone (>12 °C) and have scattered occurrence in Shrub Tundra (10–12 °C). For this period, Vorren (1978) inferred an oceanic climate with a temperature above 10° based on macrofossils of *Sphagnum papillosum* and pollen of Apiaceae and cf. *Melampyrium*, an observation he later disregarded as likely contamination or reworked material (Vorren et al., 2013). A cold period ca 16.6–17.5 cal ka BP, in which Vorren et al. (2013) recorded high frequencies of the arctic/alpine bryophyte *Aulacomnium turgidum*, falls within the hiatus in our core. Our core may therefore not cover the coldest period. However, the earlier record of Apiaceae pollen (Vorren, 1978) was confirmed by our Apiaceae *sedaDNA*. Overall, our data and review of previous records strongly suggest at least short periods with July temperatures up to 10 °C.

High nutrient input from birds may compensate for low temperatures (González-Bergonzoni et al., 2017). In addition, the southeast-facing slope of Store Æråsen, which is the closest likely site for such a bird cliff (Fig. 2), could have provided favourable microclimate, as south-facing slopes maximize sun exposure in the Arctic (Armbruster et al., 2007). Many bird cliffs in the Arctic today are south-facing, highly productive environments with rare species (svalbardflora.no). In addition, birds may also facilitate long-distance dispersal (Alsos et al., 2015). Thus, the combination of south-facing slope, nutrient input, and bird dispersal may have facilitated the presence of unusual (azonal) plant assemblages and allowed plants to grow beyond their normal temperature limit.

Picea and *Pinus* are currently scattered and rare, respectively, in Shrub Tundra (10–12 °C) (Elven et al., 2011). *Picea abies* has been reported to survive and occasionally even to produce viable seeds at mean July–August temperatures down to 5 °C (Kullman, 2002) and seeds of both *Pinus sylvestris* and *Picea abies* germinate, and may even have increased seedling survival, above the current treeline (Bougnounou et al., 2018). Recent studies have shown that nutrient availability interacts with temperature to enhance *Picea glauca* growth at the treeline in Alaska (Sullivan, 2016) and at a micro-scale to favour germination (Sullivan and Sveinbjörnsson, 2010). Thus, nutrient-rich, south-facing slopes, cliffs providing wind protection, and enhanced summer degree-day sums related to local topography, could have been relatively favourable localities for tree establishment and growth, at least during the warmest phases of LGM. Therefore, the environmental conditions based on all available evidence do not exclude local growth of *Picea* and *Pinus*, at least during short warm phases, whereas *in situ* survival during the entire LGM seems unlikely (except potentially as seeds in frozen ground).

5.4. Enrichment of the flora from 14.2 cal ka BP

A change in flora around 14.2 cal ka BP, with an increase in taxa such as*Oxyria,* has also been observed in records from the neighbouring lakes (Vorren, 1978; Vorren et al., 1988; Alm and Birks, 1991) and is associated with a change from high arctic to middle or low arctic condition (Alm, 1993 and references therein).

We observed only a minor change at the onset of the Holocene (11.7 cal ka BP), whereas the flora indicates major warming from 10.8-10.6 cal ka BP. While Øvre Æråsen and neighbouring lakes have been intensively studied for the Full and Late Glacial period, they barely include the Holocene, and sample sizes/age-depth models are poor for the transition period. Also, the nearby lake Lusvatn to the south has contaminated sediments at the transition to Holocene (Aarnes et al., 2012; Birks et al., 2014). Nevertheless, the chemostratigraphc data of lake Endletvatnet indicate that the major transition was at 10.5 cal ka BP (Vorren and Alm, 1999), corresponding to our transition for U5a to U5b at 10.6 cal ka BP. Also, available records indicate a transition to birch forest with tall forbs and ferns (Vorren, 1978; Alm, 1993; Birks et al., 2014). Further, a more detailed record from Nedre Æråsvatnet (Vorren et al., 2009) also shows a low-arctic environment prior to 11 cal ka BP, and establishment of *Betula pubescence-Filipendula* forest between 10420 and 10250 cal BP. The *sedaDNA* record is especially rich in aquatic macrophytes and spore plants, including taxa not recorded in previous pollen or macrofossil records. Moreover, while some taxa appear at about the same time in all proxies e.g. *Filipendula* and *Potamogeton,* we note that they suggest slightly different first arrival times for some key taxa such as *Salix*, *Betula* and *Vaccinium*, emphasising the advantage of using several proxies for past species distribution.

5.5. Glacial survival of plant taxa on Andøya

The presence of a *Papaver* seed in the lowermost sampled diamicton (ca. 26.7 cal ka BP) indicates that *Papaver* may have survived the last glaciation *in situ*, supporting the conclusion of Alm and Birks (1991) for *Papaver radicatum*. This is a genetically diverse genus, and the existence of a separate genetic group of *P. radicatum* in northern Norway (Solstad, 2009) also supports the glacial survival hypothesis (Brochmann et al., 2003). That hardy taxa such as *Papaver* could have persisted through both cold and warmer phases of the last glacial period on Andøya is not particularly controversial. Other arctic or low arctic species may have survived dormant as seeds or other propagules frozen in the ground, which is also a form of survival. The scattered record of more thermophilous plant species both in this and in previous records, may indicate short-term presence, which seems more likely now that we understand the high nutrient conditions supplied by the bird cliff.

6. Conclusions

New records from three cores in Øvre Æråsvatnet confirm that northern Andøya was ice-free from at least 23.4 cal ka BP and probably earlier (26.7 cal ka BP), as previously suggested by Alm (1993). Local conditions were ideal for populations of cliff-nesting seabirds. This is reflected in the Øvre Æråsvatnet stratigraphy and most clearly in stable isotope values, along with further discoveries of auk bones. The presence of thermophilous taxa in *sedaDNA* and macrofossils indicate at least short periods of Low Arctic Tundra conditions (July mean up to 8–9 °C) and possibly Shrub Tundra conditions (July mean 10–12 °C) in the period 24–14.2 cal ka BP. We did record *Pinus* and *Picea* DNA, but the frequency was so low that it could not be distinguished from background contamination. Several recorded species have climate limits similar to those of

Pinus and *Picea*. Based on this, and the local high-nutrient input, we conclude that environmental conditions, at least temporarily, would not exclude growth of pine and spruce, but we can provide no firm evidence for this. It is clear that in northern Andøya a combination of proximity to warm oceanic water, coastal nunataks and a sea-bird colony produced an environmental 'hotspot' and micro-refugia, at the edge of the Eurasian Ice sheet. This hotspot is unlikely to have been unique. While such environmental analogues do not occur today near the edge of ice sheets, these conditions may be realized in the near future with rapid ice-sheet retreat, ecological range changes and human-aided plant dispersal.

Author contributions

IGA, MEE and TA planned and designed the research; IGA, AP, LG and PS carried out the coring; JB and WGMB did the bathymetry; LG, IGA, MKFM and PS performed the *seda*DNA analysis; YL performed the bioinformatics analyses; AP and CTL performed the pollen analysis; PS performed the macrofossil analysis; PS, ML, and AGB performed the geochemical analyses; TG performed the AMS dating; IGA and AGB did the age-depth modelling; IGA, PS and TA carried out the review; IGA, AGB and PS organized the data and wrote the manuscript with major input from MEE. All co-authors commented on the manuscript.

Data availability

Raw DNA reads are uploaded at Dryad (https://doi.org/10.5061/dryad.zw3r2285q). The data obtained after filtering and taxonomic assignment are available in Supplementary Table S4.

Declaration of competing interest

Ludovic Gielly is one of the co-inventors of patents related to g-h primers and the subsequent use of the P6 loop of the chloroplast *trn*L (UAA) intron for plant identification using degraded template DNA. These patents only restrict commercial applications and have no impact on the use of this locus by academic researchers.

Acknowledgements

We thank Sandra Garces Pastor for help with the *seda*DNA analyses of run 3, Arve Elvebakk for identification of a macrofossil as *Warnstorfia fluitans*, and Charlotte Clarke and Lyn Aspden for help with figures. We thank John Lowe and an anonymous reviewer for helpful comments on the manuscript. The work was supported by the Research Council of Norway (grant nos. 213692/F20, 230617/E10 and 250963/F20) and European Research Council (ERC) under the European Union's Horizon 2020 research and innovation programme (grant agreement no. 819192) to Alsos.

Appendix A. Supplementary data

Supplementary data to this article can be found online at https://doi.org/10.1016/j.quascirev.2020.106364.

References

Aarnes, I., Bjune, A., Birks, H., Balascio, N., Bakke, J., Blaauw, M., 2012. Vegetation responses to rapid climatic changes during the last deglaciation 13,500–8,000 years ago on southwest Andøya, arctic Norway. Veg. Hist. Archaeobotany 21, 17–35.

Alm, T., 1993. Øvre Æråsvatn – palynostratigraphy of a 22,000 to 10,000 B.P. lacustrine record on Andøya, Northern Norway. Boreas 22, 171–188.

Alm, T., Birks, H.H., 1991. Late Weichselian flora and vegetation of Andøya, Northern Norway - macrofossil (seed and fruit) evidence from Nedre Æråsvatn. Nord. J. Bot. - Sect. Geobot. 11, 465–476.

Alm, T., Elverland, E., 2012. A Late Weichselian *Alle alle* colony on Andøya, northern Norway - a contribution to the history of an important Arctic environment (PhD thesis). In: Elverland, E. (Ed.), Late Weichselian to Early Holocene Vegetation and Bird Activity on Andøya, Nordland County. As Evident Primarily by Macrofossils. Univerity of Tromsø.

Alm, T., Willassen, E., 1993. Late Weichselian chironomidae stratigraphy of Nedre Æråsvatn, Andøya, northern Norway. Hydrobiologia 254, 21–32.

Alsos, I.G., Ehrich, D., Eidesen, P.B., Solstad, H., Westergaard, K.B., Schönswetter, P., Tribsch, A., Birkeland, S., Elven, R., Brochmann, C., 2015. Long-distance plant dispersal to North Atlantic islands: colonization routes and founder effect. AoB Plants 7.

Alsos, I.G., Lammers, Y., Yoccoz, N.G., Jørgensen, T., Sjögren, P., Gielly, L., Edwards, M.E., 2018. Plant DNA metabarcoding of lake sediments: how does it represent the contemporary vegetation. PloS One 13, e0195403.

Alsos, I.G., Sjögren, P., Edwards, M.E., Landvik, J.Y., Gielly, L., Forwick, M., Coissac, E., Brown, A.G., Jakobsen, L.V., Føreid, M.K., Pedersen, M.W., 2016. Sedimentary ancient DNA from Lake Skartjørna, Svalbard: assessing the resilience of arctic flora to Holocene climate change. Holocene 26, 627–642.

Anderson, L.L., Hu, F.S., Nelson, D.M., Petit, R.J., Paige, K.N., 2006. Ice-age endurance: DNA evidence of a white spruce refugium in Alaska. Proc. Natl. Acad. Sci. Unit. States Am. 103, 12447–12450.

Armbruster, W.S., Rae, D.A., Edwards, M.E., 2007. Topographic complexity and terrestrial biotic response to high-latitude climate change: variance is as important as the mean. In: Ørbæk, J.B., Kallenborn, R., Tombre, I., Hegseth, E.N., Falk-Petersen, S., Hoel, A.H. (Eds.), Arctic Alpine Ecosystems and People in a Changing Environment. Springer Verlag, Berlin.

Ballantyne, C.K., 2002. A general model of paraglacial landscape response. Holocene 12, 371–376.

Bennike, O., 1999. Colonisation of Greenland by plants and animals after the last ice age: a review. Polar Rec. 35, 323–336.

Bennike, O., Hedenäs, L., 1995. Early Holocene land floras and faunas from Edgeøya, eastern svalbard. Polar Res. 14, 205–214.

Berglund, B.E., Ralska-Jasiewiczowa, M., 1986. Handbook of Holocene Palaeoecology and Palaeohydrology. John Wiley & Sons Ltd., Chichester.

Binney, H.A., Willis, K.J., Edwards, M.E., Bhagwat, S.A., Anderson, P.M., Andreev, A.A., Blaauw, M., Damblon, F., Haesaerts, P., Kienast, F., Kremenetski, K.V., Krivonogov, S.K., Lozhkin, A.V., MacDonald, G.M., Novenko, E.Y., Oksanen, P., Sapelko, T.V., Väliranta, M., Vazhenina, L., 2009. The distribution of late-Quaternary woody taxa in northern Eurasia: evidence from a new macrofossil database. Quat. Sci. Rev. 28, 2445–2464.

Birks, H.H., 1991. Holocene vegetational history and climatic changes in west Spitsbergen - plant macrofossils from Skardtjørna, an Arctic lake. Holocene 1, 209–218.

Birks, H.H., Aarnes, I., Bjune, A.E., Brooks, S.J., Bakke, J., Kühl, N., Birks, H.J.B., 2014. Lateglacial and early-Holocene climate variability reconstructed from multi-proxy records on Andøya, northern Norway. Quat. Sci. Rev. 89, 108–122.

Birks, H.H., Birks, H.J.B., 2014. To what extent did changes in July temperature influence Lateglacial vegetation patterns in NW Europe? Quat. Sci. Rev. 106, 262–277.

Birks, H.H., Giesecke, T., Hewitt, G.M., Tzedakis, P.C., Bakke, J., Birks, H.J.B., 2012a. Comment on "Glacial survival of boreal trees in northern Scandinavia". Science 338, 742.

Birks, H.H., Jones, V.J., Brooks, S.J., Birks, H.J.B., Telford, R.J., Juggins, S., Peglar, S.M., 2012b. From cold to cool in northernmost Norway: lateglacial and early Holocene multi-proxy environmental and climate reconstructions from Jansvatnet, Hammerfest. Quat. Sci. Rev. 33, 100–120.

Birks, H.H., Larsen, E., Birks, H.J.B., 2005. Did tree-*Betula, Pinus* and *Picea* survive the last glaciation along the west coast of Norway? A review of the evidence, in light of Kullman (2002). J. Biogeogr. 32, 1461–1471.

Birks, H.J.B., Willis, K.J., 2008. Alpines, trees, and refugia in Europe. Plant Ecol. Divers. 1, 147–160.

Blaauw, M., Christen, J., 2011. Flexible paleoclimate age-depth models using an autoregressive gamma process. Bayesian Anal. 6, 457–474.

Boessenkool, S., McGlynn, G., Epp, L.S., Taylor, D., Pimentel, M., Gizaw, A., Nemomissa, S., Brochmann, C., Popp, M., 2014. Use of ancient sedimentary DNA as a novel conservation tool for high-altitude tropical biodiversity. Conserv. Biol. 28, 446–455.

Bougnounou, F., Hulme, P.E., Oksanen, L., Suominen, O., Olofsson, J., 2018. Role of climate and herbivory on native and alien conifer seedling recruitment at and above the Fennoscandian treeline. J. Veg. Sci.

Boyer, F., Mercier, C., Bonin, A., Le Bras, Y., Taberlet, P., Coissac, E., 2016. OBITOOLS: a unix-inspired software package for DNA metabarcoding. Mol. Ecol. Res. 16, 176–182.

Boyle, J.F., 2007. Loss of apatite caused irreversible early-Holocene lake acidification. Holocene 17, 543–547.

Brochmann, C., Gabrielsen, T.M., Nordal, I., Landvik, J.Y., Elven, R., 2003. Glacial survival or *tabula rasa*? The history of North Atlantic biota revisited. Taxon 52, 417–450.

Bronk Ramsey, C., 2009. Bayesian analysis of radiocarbon dates. Radiocarbon 51, 337–360.

Brubaker, L.B., Anderson, P.M., Edwards, M.E., Lozhkin, A.V., 2005. Beringia as a glacial refugium for boreal trees and shrubs: new perspectives from mapped pollen data. J. Biogeogr. 32, 833–848.

Clare, J., 2018. Daphnis: an Aquarius's Guide. V. 3.2.

Clarke, C.L., Edwards, M.E., Brown, A.G., Gielly, L., Lammers, Y., Heintzman, P.D.,

Ancin-Murguzur, F.J., Bråthen, K.-A., Goslar, T., Alsos, I.G., 2018. Holocene floristic diversity and richness in northeast Norway revealed by sedimentary ancient DNA (sedaDNA) and pollen. Boreas, 0.
Clarke, C.L., Edwards, M.E., Gielly, L., Ehrich, D., Hughes, P.D.M., Morozova, L.M., Haflidason, H., Mangerud, J., Svendsen, J.I., Alsos, I.G., 2019. Persistence of arctic-alpine flora during 24,000 years of environmental change in the Polar Urals. Sci. Rep. 9, 19613.
Eilertsen, R.S., Bøe, R., Hermanns, R., Longva, O., Dahlgren, S., 2016. Kettle holes, 'dead-ice' topography and eskers on a lake floor in Telemark, southern Norway. In: Dowdswell, J.A., Canals, M., Jakobsson, M., Todd, B.J., Dowdeswell, E.K., Hogan, K.A. (Eds.), Atlas of Submarine Glacial Landforms: Modern, Quaternary and Ancient. Geological Society of London Memoirs, pp. 113–114.
Elven, R., Murray, D.F., Razzhivin, V.Y., Yurtsev, B.A., 2011. Annotated Checklist of the Panarctic Flora (PAF). Vascular Plants. CAFF/University of Oslo, Natural History Museum, University of Oslo.
Elverland, E., 2012. Late Weichselian to Early Holocene Vegetation and Bird Activity on Andøya, Nordland County. As Evidenced Primarily by Macrofossils. University of Tromsø, Tromsø.
Elverland, E., Alm, T., 2012. High resolution macrofossil analyses of Late Weichselian Arctic lacustrine sediments on Andøya, northern Norway (PhD thesis). In: Elverland, E. (Ed.), Late Weichselian to Early Holocene Vegetation and Bird Activity on Andøya, Nordland County. As Evident Primarily by Macrofossils. Univerity of Tromsø.
Ficetola, G.F., Pansu, J., Bonin, A., Coissac, E., Giguet-Covex, C., De Barba, M., Gielly, L., Lopes, C.M., Boyer, F., Pompanon, F., Rayé, G., Taberlet, P., 2015. Replication levels, false presences and the estimation of the presence/absence from eDNA metabarcoding data. Mol. Ecol. Res. 15, 543–556.
Fjellberg, A., 1978. Fragments of a middle Weichselian fauna on Andøya, north Norway. Boreas 7, 39-39.
Fægri, K., Iversen, J., 1989. In: Fægri, K., Kaland, P.E., Krzywinski, K. (Eds.), Textbook of Pollen Analysis 4. Revised Edition. Wiley, Chichester, p. 314.
Gąsiorowski, M., Sienkiewicz, E., 2013. The sources of carbon and nitrogen in mountain lakes and the role of human activity in their modification determined by tracking stable isotope composition. Water, Air, Soil Pollut. 224, 1498.
González-Bergonzoni, I., Johansen, K.L., Mosbech, A., Landkildehus, F., Jeppesen, E., Davidson, T.A., 2017. Small birds, big effects: the little auk (*Alle alle*) transforms high Arctic ecosystems. Proc. Biol. Sci. 284.
Grønlie, A.M., 1948. The ornithocoprophilous vegetation of the bird-cliffs of Røst in the Lofoten islands, northern Norway. Nyt magazin for naturvidenskaberne 86, 117–243.
Heikkilä, M., Fontana, S.L., Seppä, H., 2009. Rapid Lateglacial tree population dynamics and ecosystem changes in the eastern Baltic region. J. Quat. Sci. 24, 802–815.
Hughes, A.L.C., Gyllencreutz, R., Lohne, Ø.S., Mangerud, J., Svendsen, J.I., 2016. The last Eurasian ice sheets – a chronological database and time-slice reconstruction, DATED-1. Boreas 45, 1–45.
Hyvärinen, H., 1970. Flandrian pollen diagrams from Svalbard. Geogr. Ann. 52 A, 213–222.
Karlsen, S.R., Elvebakk, A., 2003. A method using indicator plants to map local climatic variation in the Kangerlussuaq/Scoresby Sund area, East Greenland. J. Biogeogr. 30, 1469–1491.
Karlsen, S.R., Elvebakk, A., Johansen, B., 2005. A vegetation-based method to map climatic variation in the arctic-boreal transition area of Finnmark, northeasternmost Norway. J. Biogeogr. 32, 1161–1186.
Kullman, L., 2002. Boreal tree taxa in the central Scandes during the Late-Glacial: implications for Late-Quaternary forest history. J. Biogeogr. 29, 1117–1124.
Kullman, L., 2005. On the ocurrence of late-glacial trees in the Scandes. J. Biogeogr. 32, 1499–1500.
Kullman, L., 2006. Late-glacial trees from arctic coast to alpine tundra: response to Birks et al. 2005 and 2006. J. Biogeogr. 33, 377–378.
Laberg, J.S., Vorren, T.O., Dowdeswell, J.A., Kenyon, N.H., Taylor, J., 2000. The Andøya Slide and the Andøya canyon, north-eastern Norwegian–Greenland sea. Mar. Geol. 162, 259–275.
Lamb, H., Edwards, M.E., 1988. The arctic. In: Huntley, B., Webb, T.I. (Eds.), Vegetation History. Handbook of Vegetation Science 7. Kluwer Academic Publishers, Dordrecht, pp. 519–555.
Lammers, Y., Heintzman, P.H., Alsos, I.G., 2020. Environmental Palaeogenomic Reconstruction of an Ice Age Algal Population. https://doi.org/10.1101/2020.04.10.035535 biorxiv.org.
Larsen, E., Gulliksen, S., Lauritzen, S.-E., Lie, R., Løvlie, R., Mangerud, J., 1987. Cave stratigraphy in western Norway; multiple Weichselian glaciations and interstadial vertebrate fauna. Boreas 16, 267–292.
Mangerud, J., 2003. Ice sheet limits in Norway and on the Norwegian continental shelf. In: Ehlers, J. (Ed.), Glacial Deposits in North-West Europe. A.A. Balkema, Rotterdam, pp. 61–73.
Mangerud, J., Gulliksen, S., Larsen, E., Longva, O., Miller, G.H., Sejrup, H.-P., Sønstegaard, E., 1981. A middle Weichselain ice-free period in western Norway: the Ålesund interstadial. Boreas 10, 447–462.
Modin, H., 2016. Higher Temperatures Increase Nutrient Availability in the High Arctic, Causing Elevated Competitive Pressure and a Decline in Papaver Radicatum. Dept of Physical Geography and Ecosystem Science.
Moore, P.D., Webb, J.A., Collinson, M.E., 1991. Pollen Analysis. Blackwell Scientific Publications, Oxford.
Napier, J.D., Fernandez, M.C., de Lafontaine, G., Hu, F.S., 2020. Ice-age persistence and genetic isolation of the disjunct distribution of larch in Alaska. Ecology and Evolution. https://doi.org/10.1002/ece3.6031.
Nesje, A., 1992. A piston corer for lacustrine and marine sediments. Arct. Alp. Res. 24, 257–259.
Nesje, A., Dahl, S.O., Linge, H., Ballantyne, C.K., McCarroll, D., Brook, E.J., Raisbeck, G.M., Yiou, F., 2007. The surface geometry of the Last Glacial Maximum ice sheet in the Andøya-Skånland region, northern Norway, constrained by surface exposure dating and clay mineralogy. Boreas 36, 227–239.
Niemeyer, B., Epp, L.S., Stoof-Leichsenring, K.R., Pestryakova, L.A., Herzschuh, U., 2017. A comparison of sedimentary DNA and pollen from lake sediments in recording vegetation composition at the Siberian treeline. Mol. Ecol. Res. 17, e46–e62.
Osburn, C.L., Anderson, N.J., Leng, M.J., Barry, C.D., Whiteford, E.J., 2019. Stable isotopes reveal independent carbon pools across an Arctic hydro-climatic gradient: implications for the fate of carbon in warmer and drier conditions. Limnol. Oceanogr. Lett. 4, 205–213.
Parducci, L., Bennett, K.D., Ficetola, G.F., Alsos, I.G., Suyama, Y., Wood, J.R., Pedersen, M.W., 2017. Transley Reviews: ancient plant DNA from lake sediments. New Phytol. 214, 924–942.
Parducci, L., Edwards, M.E., Bennett, K.D., Alm, T., Elverland, E., Tollefsrud, M.M., Jørgensen, T., Houmark-Nielsen, M., Larsen, N.K., Kjær, K.H., Fontana, S.L., Alsos, I.G., Willerslev, E., 2012a. Response to comment on "glacial survival of boreal trees in northern Scandinavia". Science 338, 742.
Parducci, L., Jørgensen, T., Tollefsrud, M.M., Elverland, E., Alm, T., Fontana, S.L., Bennett, K.D., Haile, J., Matetovici, I., Suyama, Y., Edwards, M.E., Andersen, K., Rasmussen, M., Boessenkool, S., Coissac, E., Brochmann, C., Taberlet, P., Houmark-Nielsen, M., Larsen, N.K., Orlando, L., Gilbert, M.T.P., Kjær, K.H., Alsos, I.G., Willerslev, E., 2012b. Glacial survival of boreal trees in northern Scandinavia. Science 335, 1083–1086.
Patton, H., Hubbard, A., Andreassen, K., Auriac, A., Whitehouse, P.L., Stroeven, A.P., Shackleton, C., Winsborrow, M., Heyman, J., Hall, A.M., 2017. Deglaciation of the Eurasian ice sheet complex. Quat. Sci. Rev. 169, 148–172.
Paus, A., Boessenkool, S., Brochmann, C., Epp, L.S., Fabel, D., Haflidason, H., Linge, H., 2015. Lake Store Finnsjøen – a key for understanding Lateglacial/early Holocene vegetation and ice sheet dynamics in the central Scandes Mountains. Quat. Sci. Rev. 121, 36–51.
Rasmussen, T.L., Thomsen, E., Skirbekk, K., Ślubowska-Woldengen, M., Klitgaard Kristensen, D., Koç, N., 2014. Spatial and temporal distribution of Holocene temperature maxima in the northern Nordic seas: interplay of Atlantic-, Arctic- and polar water masses. Quat. Sci. Rev. 92, 280–291.
Reimer, P.J., Bard, E., Bayliss, A., Beck, J.W., Blackwell, P.G., Bronk Ramsey, C., Buck, C.E., Cheng, H., Edwards, R.L., Friedrich, M., Grootes, P.M., Guilderson, T.P., Haflidason, H., Hajdas, I., Hatté, C., Heaton, T.J., Hoffmann, D.L., Hogg, A.G., Hughen, K.A., Kaiser, K.F., Kromer, B., Manning, S.W., Niu, M., Reimer, R.W., Richards, D.A., Scott, E.M., Southon, J.R., Staff, R.A., Turney, C.S.M., van der Plicht, J., 2013. IntCal13 and Marine13 Radiocarbon Age Calibration Curves 0–50,000 Years Cal BP.
Rozema, J., Boelen, P., Doorenbosch, M., Bohncke, S., Blokker, P., Boekel, C., Broekman, R., Konert, M., 2006. A vegetation, climate and environment reconstruction based on palynological analyses of high arctic tundra peat cores (5000–6000 years BP) from Svalbard. Plants Clim. Chang. 41, 155–174.
Schenk, F, Bennike, O, Väliranta, M, Avery, R, Björk, S, Wohlfart, B, 2020. Floral evidence for high summer temperatures in southern Scandinavia during 15–11 cal ka BP. Q. Sci. Rev. 233 https://doi.org/10.1016/j.quascirev.2020.106243.
Sjögren, P., Edwards, M.E., Gielly, L., Langdon, C.T., Croudace, I.W., Merkel, M.K.F., Fonville, T., Alsos, I.G., 2017. Lake sedimentary DNA accurately records 20th Century introductions of exotic conifers in Scotland. New Phytol. 213, 929–941.
Small, D., Smedley, R.K., Chiverrell, R.C., Scourse, J.D., Cofaigh, C.Ó., Duller, G.A.T., McCarron, S., Burke, M.J., Evans, D.J.A., Fabel, D., Gheorghiu, D.M., Thomas, G.S.P., Xu, S., Clark, C.D., 2018. Trough geometry was a greater influence than climate-ocean forcing in regulating retreat of the marine-based Irish-Sea Ice Stream. GSA Bull. 130, 1981–1999.
Soininen, E.M., Gauthier, G., Bilodeau, F., Berteaux, D., Gielly, L., Taberlet, P., Gussarova, G., Bellemain, E., Hassel, K., Stenøien, H.K., Epp, L., Schrøder-Nielsen, A., Brochmann, C., Yoccoz, N.G., 2015. Highly overlapping diet in two sympatric lemming species during winter revealed by DNA metabarcoding. PloS One 10, e0115335.
Solem, J.O., Alm, T., 1994. Southwards migration of freshwater invertebrates from northern Norway. Fauna Norv. Ser. A 15, 9–18.
Solstad, H., 2009. Taxonomy and Evolution of the Diploid and Polyploid *Papaver* Sect. *Meconella* (Papaveraceae), National Scentre for Biosystematics, Faculty of Mathematics and Natural Science. University of Oslo, Oslo.
Stewart, J.R., Lister, A.M., 2001. Cryptic northern refugia and the origins of the modern biota. Trends Ecol. Evol. 16, 608–613.
Sullivan, P.F., 2016. Evidence of soil nutrient availability as the proximate constraint on growth of treeline trees in northwest Alaska: reply. Ecology 97, 803–808.
Sullivan, P.F., Sveinbjörnsson, B., 2010. Microtopographic control of treeline advance in Noatak National Preserve, northwest Alaska. Ecosystems 13, 275–285.
Sønstebø, J.H., Gielly, L., Brysting, A.K., Elven, R., Edwards, M., Haile, J., Willerslev, E., Coissac, E., Rioux, D., Sannier, J., Taberlet, P., Brochmann, C., 2010. Using next-generation sequencing for molecular reconstruction of past Arctic vegetation and climate. Mol. Ecol. Res. 10, 1009–1018.
Taberlet, P., Coissac, E., Pompanon, F., Gielly, L., Miquel, C., Valentini, A., Vermat, T., Corthier, G., Brochmann, C., Willerslev, E., 2007. Power and limitations of the chloroplast trnL (UAA) intron for plant DNA barcoding. Nucleic Acids Res. 35, e14.

Taberlet, P., Prud'Homme, S.M., Campione, E., Roy, J., Miquel, C., Shehzad, W., Gielly, L., Rioux, D., Choler, P., ClÉMent, J.-C., Melodelima, C., Pompanon, F., Coissac, E., 2012. Soil sampling and isolation of extracellular DNA from large amount of starting material suitable for metabarcoding studies. Mol. Ecol. 21, 1816–1820.

Tarasov, P., Müller, S., Andreev, A., Werner, K., Diekmann, B., 2009. Younger Dryas *Larix* in eastern Siberia: a migrant or survivor? PAGES News 17, 122–124.

Thompson, H.A., White, J.R., Pratt, L.M., 2018. Spatial variation in stable isotopic composition of organic matter of macrophytes and sediments from a small Arctic lake in west Greenland. Arctic Antarct. Alpine Res. 50, S100017.

Tjallingii, R., Röhl, U., Kölling, M., Bickert, T., 2007. Influence of the water content on X-ray fluorescence core-scanning measurements in soft marine sediments. G-cubed 8, Q02004.

Trondman, A.K., Gaillard, M.J., Mazier, F., Sugita, S., Fyfe, R., Nielsen, A.B., Twiddle, C., Barratt, P., Birks, H.J.B., Bjune, A.E., Björkman, L., Broström, A., Caseldine, C., David, R., Dodson, J., Dörfler, W., Fischer, E., Geel, B., Giesecke, T., Hultberg, T., Kalnina, L., Kangur, M., Knaap, P., Koff, T., Kuneš, P., Lagerås, P., Latałowa, M., Lechterbeck, J., Leroyer, C., Leydet, M., Lindbladh, M., Marquer, L., Mitchell, F.J.G., Odgaard, B.V., Peglar, S.M., Persson, T., Poska, A., Rösch, M., Seppä, H., Veski, S., Wick, L., 2015. Pollen-based quantitative reconstructions of Holocene regional vegetation cover (plant-functional types and land-cover types) in Europe suitable for climate modelling. Global Change Biol. 21, 676–697.

Tzedakis, P.C., Emerson, B.C., Hewitt, G.M., 2013. Cryptic or mystic? Glacial tree refugia in northern Europe. Trends Ecol. Evol. 28, 696–704.

van der Bilt, W.G.M., Lane, C.S., 2019. Lake sediments with Azorean tephra reveal ice-free conditions on coastal northwest Spitsbergen during the Last Glacial Maximum. Sci. Adv. 5, eaaw5980.

van der Knaap, W.O., 1988. A pollen diagram from Brøggerhalvøya, Spitsbergen: changes in vegetation and environment from ca. 4400 to ca. 800 B.P. Arct. Alp. Res. 20, 106–116.

Vorren, K.D., 1978. Late and middle Weichselian stratigraphyof Andøya, north Norway. Boreas 7, 19–38.

Vorren, K.D., Alm, T., 1999. Late Weichselian and Holocene environments of lake Endlevatn, Andøya, northern Norway: as evidenced prilimarily by chemo-stratigraphical data. Boreas 28, 505–520.

Vorren, K.D., Elverland, E, Blaauw, M, Ravna, E.K, Jensen, C.A.H., 2009. Vegetation and climate c. 12 300–9000 cal. yr BP at Andøya, NW Norway. Boreas 38, 401–420. https://doi.org/10.1111/j.1502-3885.2008.00081.x.

Vorren, T.O., Plassen, L., 2002. Deglaciation and palaeoclimate of the Andfjord-Vågsfjord area, north Norway. Boreas 31, 97–125.

Vorren, T.O., Rydningen, T.A., Baeten, N.J., Laberg, J.S., 2015. Chronology and extent of the Lofoten–Vesterålen sector of the Scandinavian ice sheet from 26 to 16 cal. Ka BP. Boreas 44, 445–458.

Vorren, T.O., Vorren, K.-D., Aasheim, O., Dahlgren, K.I.T., Forwick, M., Hassel, K., 2013. Palaeoenvironment in northern Norway between 22.2 and 14.5 cal. ka BP. Boreas 876–895.

Vorren, T.O., Vorren, K.-D., Alm, T., Gulliksen, S., Løvlie, R., 1988. The last deglaciation (20,000 - 11,000 B.P.) on Andøya, Northern Norway. Boreas 17, 41–77.

Walker, D.A., Raynolds, M.K., Daniels, F.J.A., Einarsson, E., Elvebakk, A., Gould, W.A., Katenin, A.E., Kholod, S.S., Markon, C.J., Melnikov, E.S., Moskalenko, N.G., Talbot, S.S., Yurtsev, B.A., 2005. The circumpolar arctic vegetation map. J. Veg. Sci. 16, 267–282.

Weltje, G.J., Tjallingii, R., 2008. Calibration of XRF core scanners for quantitative geochemical logging of sediment cores: theory and application. Earth Planet Sci. Lett. 274, 423–438.

Westergaard, K.B., Zemp, N., Bruederle, L.P., Stenøien, H.K., Widmer, A., Fior, S., 2019. Population genomic evidence for plant glacial survival in Scandinavia. Mol. Ecol. 28, 818–832.

Willerslev, E., Davison, J., Moora, M., Zobel, M., Coissac, E., Edwards, M.E., Lorenzen, E.D., Vestergard, M., Gussarova, G., Haile, J., Craine, J., Gielly, L., Boessenkool, S., Epp, L.S., Pearman, P.B., Cheddadi, R., Murray, D., Bråthen, K.A., Yoccoz, N., Binney, H., Cruaud, C., Wincker, P., Goslar, T., Alsos, I.G., Bellemain, E., Brysting, A.K., Elven, R., Sonstebo, J.H., Murton, J., Sher, A., Rasmussen, M., Ronn, R., Mourier, T., Cooper, A., Austin, J., Moller, P., Froese, D., Zazula, G., Pompanon, F., Rioux, D., Niderkorn, V., Tikhonov, A., Savvinov, G., Roberts, R.G., MacPhee, R.D.E., Gilbert, M.T.P., Kjaer, K.H., Orlando, L., Brochmann, C., Taberlet, P., 2014. Fifty thousand years of Arctic vegetation and megafaunal diet. Nature 506, 47–51.

Yoccoz, N.G., 2012. The future of environmental DNA in ecology. Mol. Ecol. 21, 2031–2038.

Zazula, G.D., Telka, A.M., Harington, C.R., Schweger, C.E., Mathewes, R.W., 2006. New spruce (*Picea* spp.) macrofossils from Yukon Territory: implications for late pleistocene refugia in eastern Beringia. Arctic 59, 391–400.

Zimmermann, H.H., Raschke, E., Epp, L.S., Stoof-Leichsenring, K.R., Schwamborn, B., Schirrmeister, L., Overduin, P.P., Herzschuh, H., 2017. Sedimentary ancient DNA and pollen reveal the composition of plant organic matter in Late Quaternary permafrost sediments of the Buor Khaya Peninsula (north-eastern Siberia). Biogeosciences 14, 575–596.

Zinger, L., Bonin, A., Alsos, I.G., Bálint, M., Bik, H., Boyer, F., Chariton, A.A., Creer, S., Coissac, E., Deagle, B.E., De Barba, M., Dickie, I.A., Dumbrell, A.J., Ficetola, G.F., Fierer, N., Fumagalli, L., Gilbert, M.T.P., Jarman, S., Jumpponen, A., Kauserud, H., Orlando, L., Pansu, J., Pawlowski, J., Tedersoo, L., Thomsen, P.F., Willerslev, E., Taberlet, P., 2019. DNA metabarcoding—need for robust experimental designs to draw sound ecological conclusions. Mol. Ecol. 28, 1857–1862.